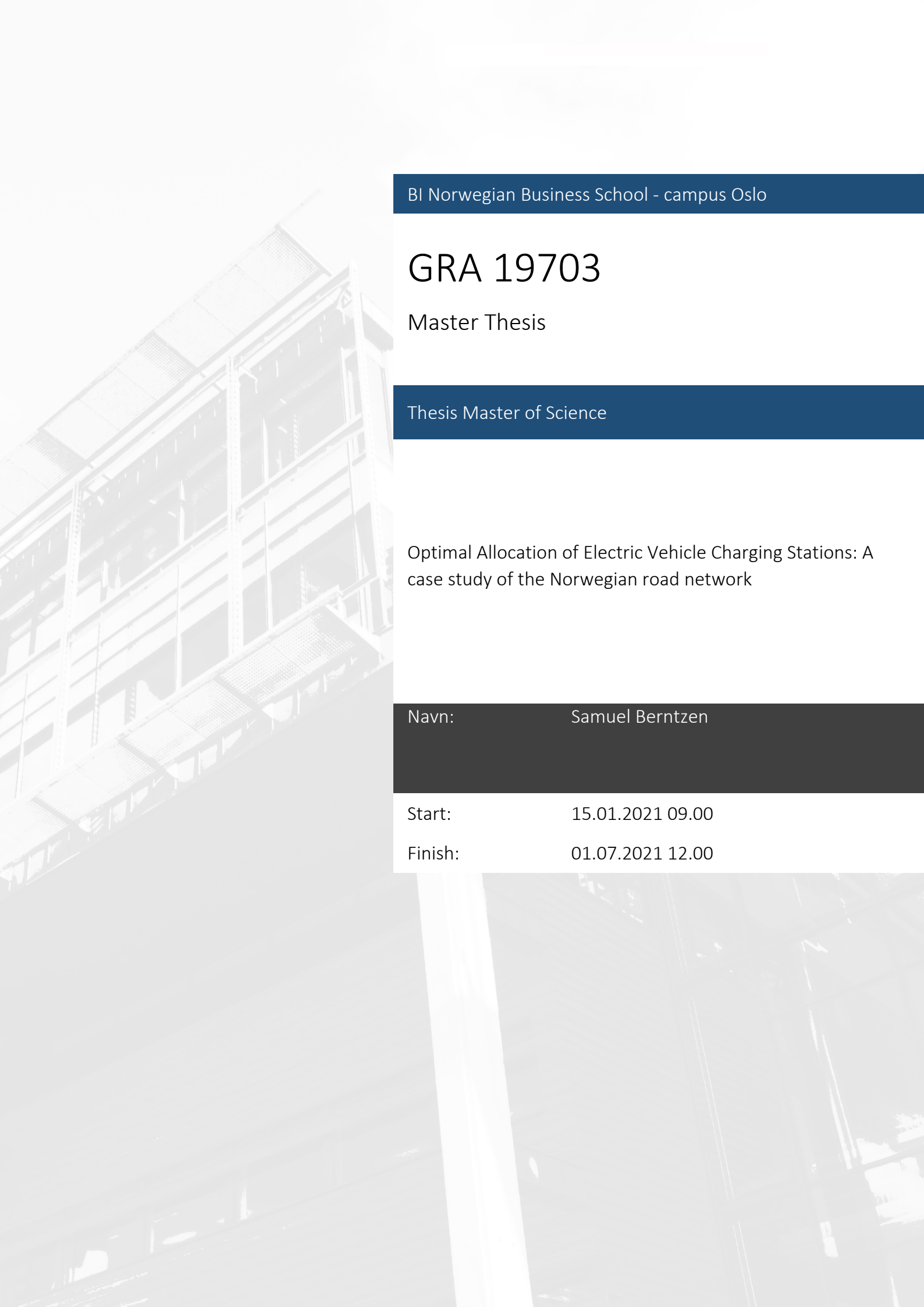

BI Norwegian Business School - campus Oslo

GRA 19703

Master Thesis

Thesis Master of Science

Optimal Allocation of Electric Vehicle Charging Stations: A case study of the Norwegian road network

Navn:	Samuel Berntzen

Start:	15.01.2021 09.00
Finish:	01.07.2021 12.00

Optimal Allocation of Electric Vehicle Charging Stations: A case study of the Norwegian road network

Master Thesis

Author
Samuel Berntzen
samuel.berntzen@protonmail.com

Supervisor
Karim Tamssaouet, BI Norwegian Business School
karim.tamssaouet@bi.no

Co-supervisor
Johannes Langguth, Simula Research Laboratory
langguth@simula.no

A thesis submitted for the degree of
Master of Science in Business Analytics

Department of Accounting, Auditing and Business Analytics

BI Norwegian Business School

Spring 2021

June 25, 2021

Abstract

Allocating fast charging stations for electric vehicles will be an important component for ensuring the adoption of electric vehicles. This thesis proposes a framework for ensuring *reachability*, meaning that all parts of the road network should be accessible with a specific battery capacity. Two methodologies are tested: (1) a *k-Dominating Set* with half range, and (2) a *Connected k-Dominating Set* for ensuring connectivity, both are tested on a dataset representing the Norwegian road network. Distance metrics are measured in kWh for an accurate representation of battery consumption. Tested ranges are 20, 30, and 40 kWh, each tested with k ranging from 1 to 4.

The experiment finds that the connected k-dominating set, computed using a greedy algorithm, provides more efficient and desirable solutions than the *k-dominating set* when applied to this problem. A simple comparison of the current system and a *connected k-dominating set* for 20 kWh and $k = 2$ finds that the current charging station allocation in Norway is not sufficient for ensuring reachability with a 20 kWh electric vehicle, and that remote, non- urban areas are especially underrepresented in terms of coverage. Because many parts of the country are already covered, future allocation of fast charging stations should occur in those that currently have low or no coverage in order to stimulate the adoption of electric vehicles.

Acknowledgements

I first and foremost want to thank my supervisor Karim Tamssaouet, assistant professor at BI Norwegian Business School, for his support, patience, and guidance throughout this thesis. Additionally, I would like to thank my co-supervisor Johannes Langguth, research scientist at Simula Research Laboratory, for giving me the opportunity to work on this topic, and for his healthy input and expertise on the subject.

I also want to thank some of my co-students, especially Abhijeet, for helpful input, discussions, and feedback.

I appreciate the support of my partner, Madeleine, for her encouragement and who patiently listened through all my ranting and complaining on evening walks with our dog.

Lastly, thank you to all proof readers who made me realize that my grammar was worse than I initially thought.

Contents

List of Figures

List of Tables

List of Algorithms

1 Introduction

This chapter presents the background and motivation of the topic, defines the research question and the problem statement.

1.1 Background

In 2016, Norway ratified the Paris Climate Accord (PCA), which provides the country with a binding legislature to reduce carbon emissions by 40% of 1990-levels, within 2030 (Norwegian Ministry of Climate and Environment, 2016). This is an ambitious goal that will require a drastic reduction of carbon dioxide emissions in every sector, the transportation sector being one of them.

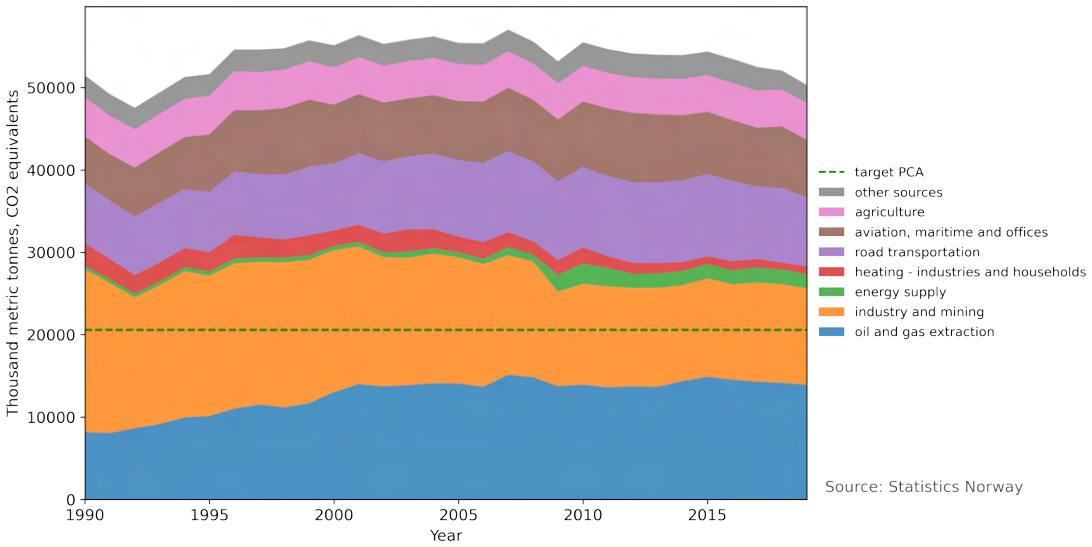

Figure 1.1: Total carbon emissions by sector, Norway

As illustrated in Figure 1.1 above, road transportation in 2019 accounted for roughly 16.6% of Norwegian carbon emissions. This is equal to 8 358 000 metric tonnes of carbon dioxide equivalents (Statistics Norway, 2020b). It is therefore not surprising that reducing emissions from the road transportation sector could play a large part in reducing Norwegian emissions overall. Electrification of vehicles could therefore be a viable option for emission reduction. As a result, the

government's *National Transportation Plan* has as a goal that every new registered passenger vehicle will be zero-emission in operation by 2025 (Ministry of Transport, 2017). However, this comes with certain challenges.

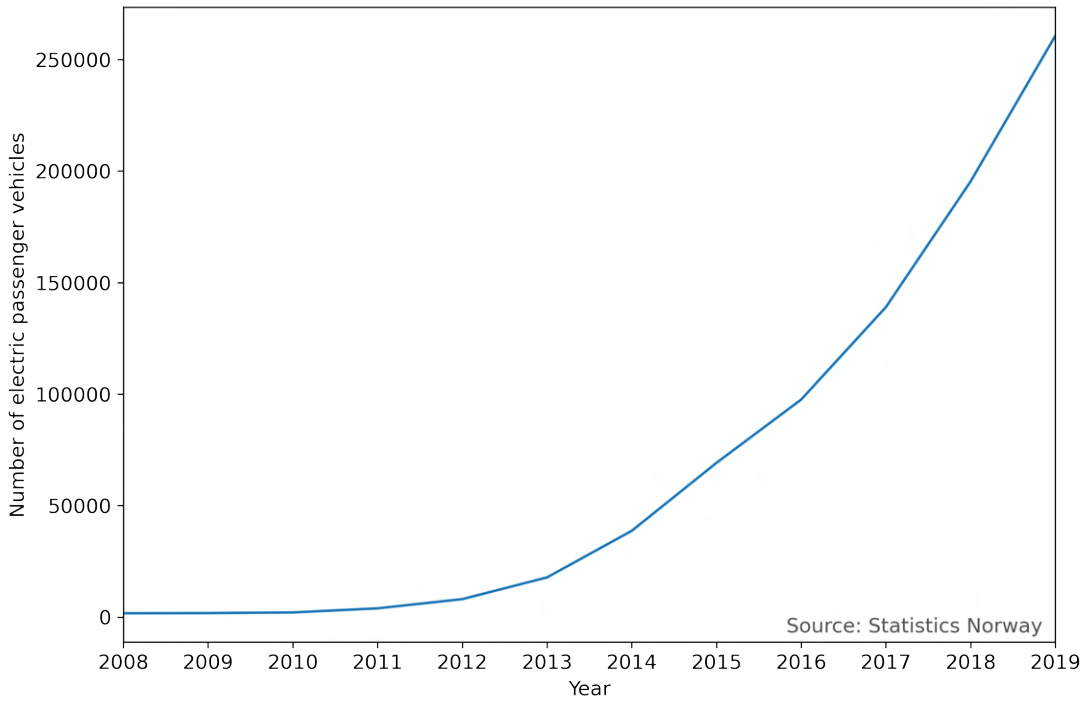

Figure 1.2: Total electric passenger car registered in Norway

Due to favorable tax and toll laws, and cheap electricity, the sale and registration of electric passenger vehicles has grown rapidly since 2008. However, these registrations are mainly located in urban counties like Oslo, Bergen, Bærum, Trondheim, and Stavanger, which represent roughly 42.5% of the total electric vehicles in the country (Statistics Norway, 2020a). The reason for this can be range issues and charging station availability. Since 2012, the rate at which regular[1] charging stations are built has been trailing behind the inflow of registered electric vehicles in the country.

Generally, electric vehicle charging stations are a nonissue for urban and short distance travels as one is able to charge the vehicle at home, which is what the

[1]Regular being non- proprietery charging stations, e.g.: Non-tesla, non-chademo 50kw+, non-ccs 50kw+

majority of people do (Figenbaum, 2019). However, charging an electric vehicle can create significant delays in one's schedule if travelling for longer distances. This phenomenon was observed during the summer of 2020, when most Norwegians remained in Norway for their vacations (Rangnes, 2020), and many electric vehicle owners experienced queuing at the charging stations. Figenbaum and Nordbakke argue that *long distance travel is one of the last hurdles for mass adoption* of electric passenger vehicles (Figenbaum, 2019).

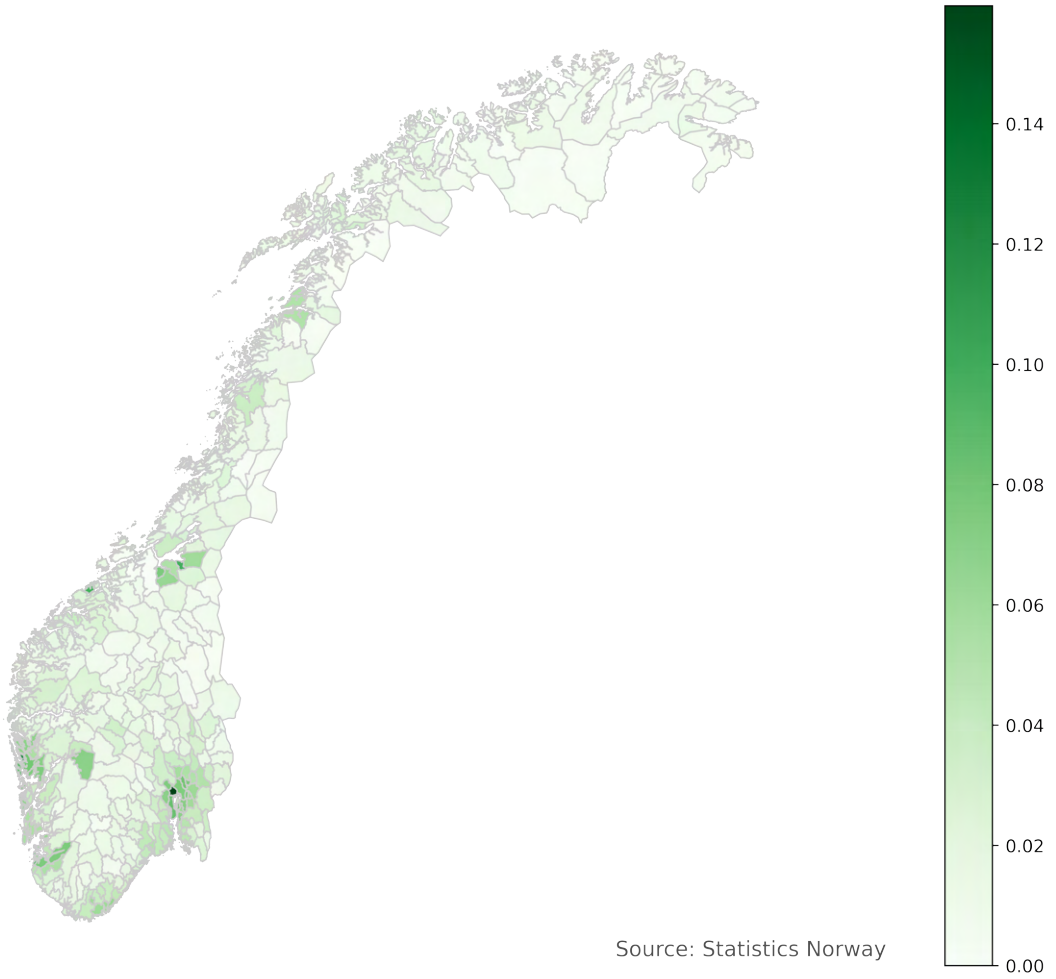

Figure 1.3: Geospatial distribution of EV per inhabitant

This skewed distribution is evident from Figure 1.3, where the green shades show the electric vehicles per inhabitant for each municipality in Norway. It is clear that urban areas such as Oslo, Bærum, Trondheim, Bergen, Stavanger, and Kris-

tiansand have a much higher concentration than all other areas of the country.

For this reason, increasing the availability of charging stations could increase the demand for electric vehicles and therefore also help in the electrification of the road transportation sector. In turn, this could also help curb Norwegian carbon emissions from the transportation sector.

1.2 Research Questions and Problem statement

Multiple researchers have compared the interaction between charging station availability and demand for electric vehicle as the *chicken-and-the-egg* problem (Upchurch & Kuby, 2010; Chung & Kwon, 2015). This paper assumes that a certain level of infrastructure is required for a demand of electric vehicles to occur. This thesis seeks to address the problem of charging station allocation by using openly available data and incorporating certain realistic elements into the dataset.

Only fast charging stations are considered for this research. The reason for this is that fast charging stations directly compete with the swiftness of refueling fossil-based vehicles, and that short distance travel can arguably be covered by charging at source and target locations. Hence, for long distance travel, fast charging stations will be the most feasible option. As a result, any reference to *charging stations* refers to fast charging stations unless otherwise specified. Secondly, parts of the Norwegian landscape are characterized by mountain ranges, meaning that the range of electric vehicles can be significantly affected by the road gradients. This should also be accounted for when allocating charging stations.

The minimum battery capacity considered reflects the battery capacities of small electric vehicles with limited range, such as the *Honda Fit*, which are often used in cities. The low end of this spectrum is around 20 kWh. Other battery capacity considered reflects the capacities of some higher end vehicles, such as the *Nissan Leaf* and *BMW i3*, which have capacities of 30 and 40 kWh, respectively. Generally, one can assume that short-range electric vehicles are cheaper than long-range

vehicles, which can make short-range vehicles more economically feasible.

Additionally, the thesis compares the current fast charging station locations with a proposed solution given by the experiments performed. This can put the current state of the system into perspective and help decision- and policymakers make a more informed decision on where future fast charging stations should be located.

1.3 Research Contribution of the Thesis

This thesis presents a framework for allocating charging stations on a national level, such that any vehicle with a minimum specified capacity can reach any location in the country from any other given location. Additionally, the thesis presents a greedy algorithm for finding a *connected k-dominating set,* which is a method that selects a set of vertices such that all vertices in the graph are k-dominated, while the induced subgraph of the dominating set is connected.The value of k signifies the criteria for domination. This means that for a vertex to be dominated, it needs to be adjacent to k vertices in the solution set. In the case of this specific problem, k would signify the number of charging stations available to a driver at each vertex. The connected k-dominating set problem has, at the time of writing, seemingly not been applied to charging station allocation.

2 Literature Review

This section gives a brief introduction to the field of facility location and location problems used for charging station locations and presents a review of work relevant to charging station allocation performed by other researchers.

Pagany et al. (2019) conducted a literature review of the current methodologies for localization of charging infrastructure. They find that the research within this subject has increased dramatically in the previous years, from near 0 published papers in 2006 to more than 120 publications in 2016 (Pagany, Camargo,

& Dorner, 2019). The authors argue that most studies on the issue are highly data-driven, but that the lack of data is an obstacle in nearly all cases. Hence, many researchers are limited to where the data availability is high, such as taxi data, if they seek to use real observations. An alternative is to upscale or make assumptions from other data sources, such as *Origin-Destination* (OD) pairs from traffic monitoring. One final issue addressed is that of the geographical research area, which the authors argue is focused around urban areas and lacking in more rural areas.

2.1 Facility Location Problems

Optimization for facility location purposes has its roots in 1909 when Alfred Weber developed a model to minimize the total distance between the warehouse and the customers (Owen & Daskin, 1998; Alfred, 1929). The research field gained traction during the 1960s following Seifollah L. Hakimi's publication on *minimax* optimization for switching centers in communication networks and police station location on a highway system (Owen & Daskin, 1998; Hakimi, 1964) using a *vertex k-center* problem. The vertex k-center problem assigns vertices to a set C such that the cardinality of that set, $|C|$, is at most equal to k, while minimizing the maximum distance to the closest selected vertex.

The *Set Covering Problem (SCP)* is also a classic location model with many applications. The SCP allocates facilities, where each facility is connected to a set of vertices, so that all vertices are covered by a facility. For instance, the SCP has been applied for determining the location of Covid-19 swab centers in city of Bandung, Indonesia. Researchers used an *integer linear program*, a mathematical representation of the problem consisting of binary in- and outputs, and some weighted variables for allocating the swab stations across the city (Muttaqin, Finata, & Masturo, 2020).

One final classic location problem addressed in this review is the *p-median problem* (PMP). Similar to the SCP, the PMP allocates facilities to a network. However,

the PMP allocates p facilities while minimizing the *demand weighted average distance* (Daskin & Maass, 2015, p.21). For instance, the PMP problem has been applied for proposing an allocation of students to facilities that are closest to their homes at the *Federal University of Paraná* in Brazil (Correa, Steiner, Freitas, & Carnieri, 2004).

2.2 Flow-Based Models

In 1990, Hodgons developed the *Flow-Capturing Location Model (FCLM)* as an alternative to *set-covering* and *maximal-covering location models* (Hodgson, 1990). The FCLM seeks to maximize the captured flow between origin-destination using *mixed integer linear programming* (MILP). Hodgons' model defines a flow f_q between O-D pair q as *captured* if there is at least one facility k along the flow's path. The objective function that maximizes the captured flow is constrained by a predefined number of facilities. While Hodgons' model is originally intended for facilities like chain stores or billboards, it has later been expanded upon for other purposes.

Kuby and Lim (2005) developed the *Flow-Refueling Location Model (FRLM)* based on the FCLM. However, while Hodgons' FCLM defines a flow as covered when only one facility is located along its path, the FRLM allows *double-counts* to occur to accommodate for the vehicle range (Kuby & Lim, 2005). Kuby and Lim show that decreasing the model's vehicle range leads to a lack of convexity and their exact solution plateaus at around 70% flow coverage, meaning that no solution satisfying all O-D flows is found. Therefore, they argue that the vehicle range should be long enough to traverse the longest edge on any shortest path in the graph. Similar to Hodgons' FCLM, their objective function is to maximize the captured flow. However, this is subject to a few more constraints such as range limitations for a flow and refuel site, and that refuel sites along a flow are only open if the entire flow is covered.

One drawback of these models is that they are assumed to be uncapacitated;

meaning that one station is sufficient to serve the entire flow. For this reason, Upchurch, Kuby, and Lim (2009) developed the *Capacitated Flow Refuel Location Model (CFRLM)*, which accounts for refuel capacity at the facilities. Their formulation of the CFRLM transforms a previously binary variable indicating if a facility is placed, to an integer variable denoting the number of facilities to place. They expand on the model to include a capacity constraint which limits the size of the flow one single refuel station can handle. The CFRLM is applied to a simplified version of the Arizona highway network, in which they estimate the O-D pairs through a *gravity model* based on population density. The gravity model, similar to Isards (1954) *gravity model of trade*, assigns traffic volume to O-D pairs based on the population between each origin and destination, so that high population vertices attract higher traffic flows. The authors solved this problem using a simple greedy heuristic (Upchurch, Kuby, & Lim, 2009).

However, as pointed out by Kuby and Lim (2010), the FRLM (and CFRLM) allows for such numerous combinations to be explored that even graphs with a few hundreds vertices make the algorithm computationally expensive. Thus, for larger graphs, they show that *greedy-adding, greedy-adding with substitution and genetic algorithms* are effective ways of finding feasible solutions for the FRLM problem. They found that the genetic algorithm had slightly better solutions at the cost of longer run times (Lim & Kuby, 2010).

Jochem et al. (2019) apply a FRLM related model to a graph representing the road network of the European Union. Due to the size of the data representing the European road network, they limit the optimization algorithm to highways in Central Europe only. An optimal solution to the problem is found in five hours (Jochem, Szimba, & Reuter-Oppermann, 2019).

A similar approach is also performed by He et al. (2019) for assigning charging stations across the United States, where instead of maximizing the covered flows, the authors rather seek to maximize the share of fulfilled completed O-D trips. To reduce the dimensionality of the data, the authors performs k-means clustering on

the graph and reduce the number of vertices from 4486 to 200 cluster centroids, from which the shortest path is subsequently found. Solutions to 30 different problem variations are found in about six hours (He, Kockelman, & Perrine, 2019).

Kuby and Kim (2012) have also expanded upon the Flow-Refuel Location Model by accounting for driver deviation from the shortest path for refuel purposes. This model is referred to as the *Deviation-Flow Refuel Location Model (DFRLM)* (Kim & Kuby, 2012). A penalty function is added, so that the objective function is penalized when the deviation from the shortest path increases, which is shown to affect the optimal location of the stations. The authors acknowledge that the application of such a model to a real-life network is limited.

2.3 Demand Weighted Approaches

While the FRLM is a commonly used model for allocating refueling facilities, other approaches more similar to the *set-cover problem* have also been performed. Lam et al. (2014) formulates an MILP model for allocating charging stations to vertices given a demand present in those vertices. They show their model to be NP-hard and apply it to a graph representing the Hong Kong area. They propose four different heuristic algorithms to solve the problem, each with different performance depending on data availability, data complexity, solution quality, and algorithmic efficiency (Lam, Leung, & Chu, 2014).

Bougera and Layeb (2019) present different models for minimizing the cost of deploying charging stations in Tunis, Tunisia. One of their capacitated models ensures that each vehicle is assigned a charging station within an acceptable driving range, thus allowing the model to accommodate for charging demand. They show that higher charging times (e.g., like deploying charging stations that are not fast chargers) increase the number of charging stations required (Bouguerra & Bhar Layeb, 2019).

Efthymiou et al. (2017) estimate O-D pairs using traffic counts and simulations,

and develop a genetic algorithm to optimally allocate charging stations across Thessaloniki, Greece. Their genetic algorithm, similar to a p-median problem, allocates a given number of charging stations across a set of candidate vertices while maximizing the covered demand. Under the assumption that 5% of vehicles will be electric, they found that 15 stations in Thessaloniki are sufficient to cover 80% of the expected demand by 2020 (Efthymiou, Chrysostomou, Morfoulaki, & Aifantopoulou, 2017).

Upchurch and Kuby (2010) compared the performance of *p-median* and *FRLM*. The p-median problem allocates p facilities and demand vertices to the facilities and minimized the distance traveled from the demand vertex to facility. They analyze how the solutions of each model perform on the other's objective function. The conclusion is that the FRLM's solutions perform better on the p-median's objective function than the p-median's solutions on the FRLM objective (Upchurch & Kuby, 2010).

2.4 Ensuring Reachability Across a Network

The approaches above take into account the traffic data or demand present in different vertices or along specific paths. However, they do not take into account *reachability* across the graph; that there is guaranteed to exist a feasible path, given a range r, from any vertex i to any other vertex j. The following section describes possible approaches for addressing reachability.

Corcoran and Gagarin (2018) developed a model for optimally allocating charging stations using a multiple domination model which guarantees reachability across the entire graph and minimizes charging related detours (Gagarin & Corcoran, 2018). Their model accounts for drivers' desire to avoid detours for charging purposes and their charging threshold[2]. They apply their model on high-dimensional graphs representing the cities of Boston and Dublin, and solve the problem by specifying it as a *k-dominating set problem*. Because the minimal k-dominating set

[2]The battery level at which drivers are likely to charge their car

problem is NP-complete, three different heuristics for ensuring reachability within a threshold of t are presented; *(1) Randomized k-dominating set, (2) Greedy k-dominating set*, and a final algorithm to remove redundant dominating vertices; *(3) Minimal k-dominating set*.

Similar methods are applied by Storandt et al. (2015), in which a model for charging station allocation is modelled as a *Hitting Set Problem*. The hitting set problem seeks to minimize the cardinality of a subset $L \subseteq V(G)$ such that, given a collection of subsets of all graph vertices Σ, L intersects every set in Σ. In this case, Σ represents the vertex-sets of every shortest path for a specific battery capacity. Their approach avoids driver detours for reaching charging stations. Their proposed model is applicable on country-sized graphs using a greedy heuristic algorithm, and a solution for a graph representing the road network of Germany was found within a *few* hours. Their approach allows for charging stations to not be placed directly on the shortest path, but rather near the path, thus reducing charging related detours (Funke, Nusser, & Storandt, 2015).

2.5 General Challenges and Constraints

Overall, there are multiple constraints and challenges to consider when allocating charging stations. As argued by Pagany et al. (2019), and previously mentioned in this section, data availability is one overarching problem for most experiments. However, as presented in this literature review, the constraints considered heavily affect the type of optimization to perform. Combining both capacity and reachability, meaning that the model should minimize or eliminate waiting times and guarantee reachability across a network, requires highly detailed data on traffic flows, the battery *State of Charge* and distances. Some models, such as the *CFRLM* (Lim & Kuby, 2010) previously presented in the section, combines capacity and traffic flow, thus maximizing, not guaranteeing, reachability and minimizing overloads. However, due to the large number of possible combinations, the CFRLM is very computationally expensive to perform on large networks (Lim

& Kuby, 2010). Additionally, for realistic results, the data can include elevation, temperature, vehicle weight, road quality, and so forth. This means that combining models for computing both reachability and elimination of waiting times is highly challenging.

3 Methodology and Data Collection

This chapter explains the methodology and data collection used for this thesis. The first part presents the research methodology and strategy used, while the final part discusses the available data and data used for the analysis.

3.1 Research Design

This thesis primarily employs a quantitative research design. While the data transformation and modeling part are clearly quantitative processes, a certain degree of qualitative research needs to be performed to gain an adequate understanding of the current needs present for both electric vehicle users and policy-makers. As such, part of the findings from the qualitative research is *translated* into quantitative abstractions such as model constraints.

The purpose of this thesis is to use the existing theory and apply it to the case of the Norwegian road network. Although the models from the theory are already often put to use for similar purposes, namely, alternative fuel station allocation, few of these are applied to country-wide datasets. Moreover, this thesis offers a prescriptive analysis of how the state of the system *should* be for charging stations to guarantee reachability across a road network representing the most important roads in Norway.

3.2 Data Collection

Data was collected using a collection of open data sources. First and foremost, the data has been collected from the Norwegian Public Roads Administration (NPRA) own data set for their vehicle routing services: *National Roads Database — Road Network for Routing* (NRDB), found on *GeoNorge* (GeoNorge, 2021). This dataset contains details such as road class, latitude and longitude, road length and road name. Additional elevation data for the road network was retrieved from the Google Map API using the *OSMnx* Python library, which is a Python framework used for geospatial graph analysis (Boeing, 2021). Data for existing charging stations are retrieved from OpenChargeMap's public database (OpenChargeMap, 2021). From this dataset, all Norwegian fast charging stations were retrieved. The choice of charging station type is motivated by the constraints previously described in the problem statement.

3.2.1 Data Preparation

The routable road data retrieved from the NPRA was first processed and filtered in QGIS, an open source software used for geospatial analysis, before it was exported in to *GeoJson* format. The filtering selects the roads up to a certain *functional road class*, so that only main[3] roads were included in the dataset. By using *NetworkX*, a Python library for studying and manipulating graphs, the GeoJson file was transformed into a graph object consisting of more than 140 000 vertices and edges.

Because the road's gradient has a profound impact on the vehicle's energy consumption (K. Liu, Yamamoto, & Morikawa, 2017), it must be considered in this experiment. The elevation of each vertex is retrieved through the Google Maps API. The edge gradient is subsequently calculated using the vertex elevation and edge direction. To clarify, the edge gradient represents the number of meters, one moves upwards, per meter moved horizontally. Thus, an edge gradient of 8%

[3]Functional road class 0 to 3, which signifies highways, trunk roads and primary roads

signifies that the vehicle will change its elevation by 8% of its traversed horizontal distance. Similarly, an edge gradient of $> 100\%$ means that the number of units moved vertically will be higher than the units moved horizontally.

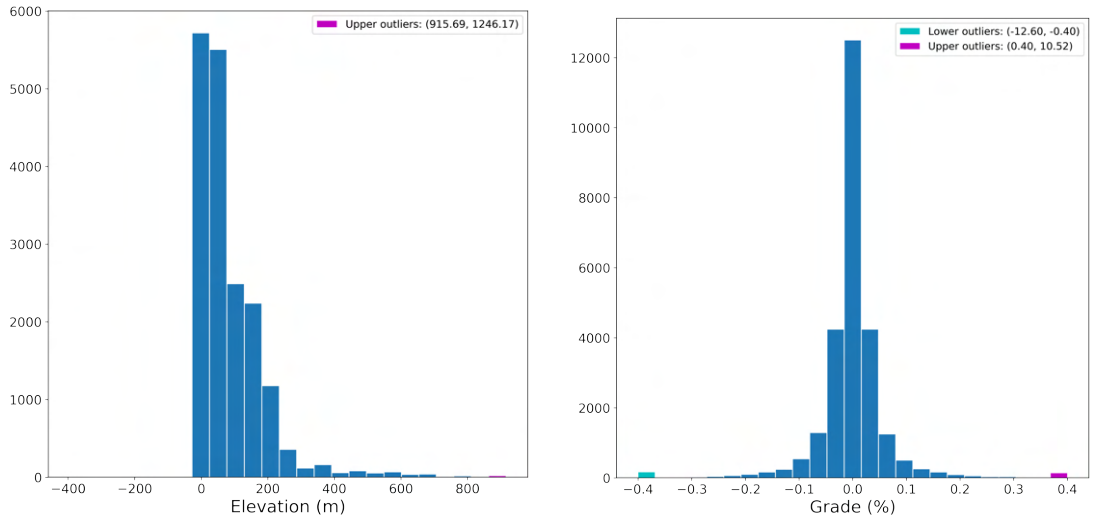

Vertex elevations

Edge gradients

Figure 3.1: Vertex elevation and edge grades distribution, with binned outliers

Figure 3.1 shows that there are certain outliers present in the distribution of edge gradients. Most notably, the steepest roads have a gradient of -12.60 and 10.52. These are errors due to inaccuracies in the API or minor deviations in the coordinates passed to the API query. However, as seen in figure 3.2 below which plots the absolute gradient value and length of the edges, the edges containing extreme values are few and are short. Therefore, their impact is very limited.

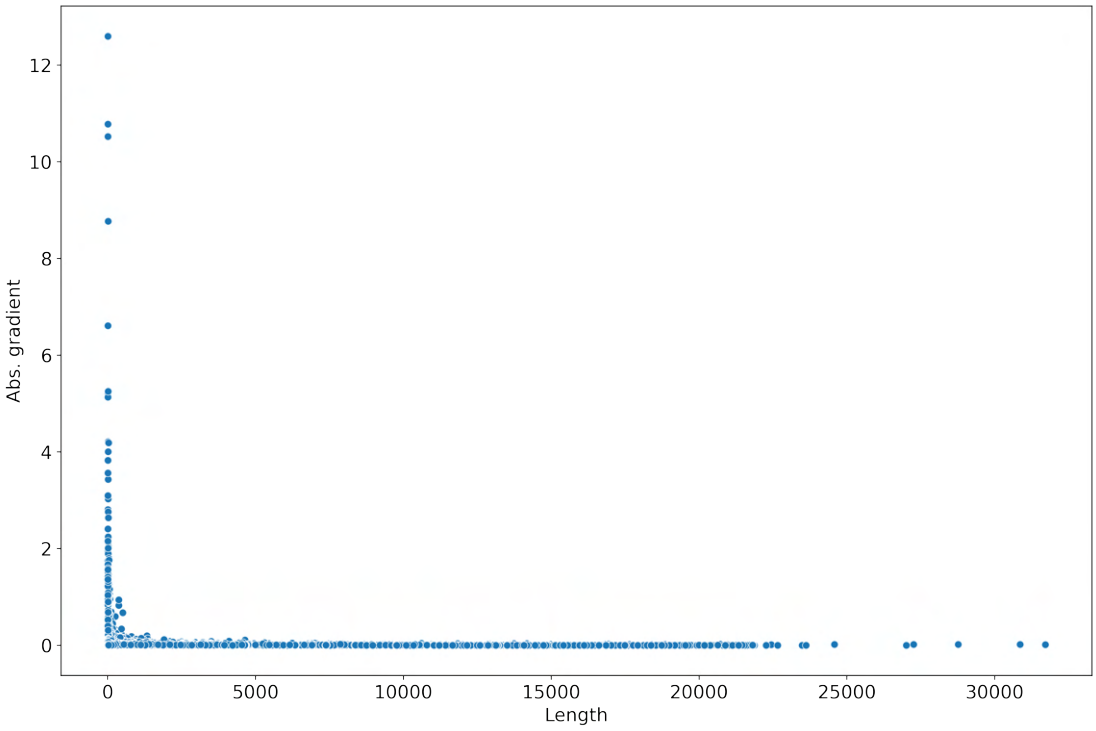

Figure 3.2: Absolute gradient and edge length

In the original graph, vertices represent crossroads, dead ends, rest areas, and so forth, but many vertices also represent curves in the road and are therefore not very useful. Thus, after the grade and elevation have been computed, a graph operation referred to as *simplification* is performed. This process removes any interstitial vertices, such that only dead ends and crossroads are kept. One issue that arises as a result of the simplification process is that the edge grade and edge length will not be as accurate as with a high-resolution graph. The process of estimating the grade for the simplified edges starts during the simplification process, where the collection of grades and lengths along a simplified edge are inserted into the arrays H and L respectively and stored as a separate variable. Using H and L, the weighted average grade between vertex u and v, $g^w_{u,v}$, is calculated for each simplified edge:

$$g^w_{u,v} = \frac{\sum_{i=1}^{n} L_i * H_i}{\sum_{i=1}^{n} L_i}$$

Where the array of lengths L_i functions as the weight of each observed grade in H.

Through the use of GPS tracking and *state of Charge (SoC)* reporting, Liu et al. (2017) estimated the effect of road gradient on electric vehicle average energy consumption. Their research studied 492 electric vehicles across different brands, weights, and weather conditions. They propose a linear regression model with fixed effect for estimating the excess energy consumption of each interval of road gradient. Their findings are presented in Table 3.1 below as kilowatt hours (kWh) per kilometer:

Ind. variable	Coefficient, kWh per kilometer
Constant β_0	0.372
$< -9\%$	-0.332
[-9% -7%)	-0.217
[-7% -5%)	-0.148
[-5% -3%)	-0.121
[-3% -1%)	-0.073
[1% 3%)	0.085
[3% 5%)	0.152
[5% 7%)	0.203
[7% 9%)	0.306
[9% 11%)	0.358
$> 11\%$	0.552

Table 3.1: Gradient impact on kWh consumption (Liu et al., 2017) (excerpt)

Using the values in Table 3.1, the weighted- and regular grade, and edge length, one can estimate the average kWh consumption for traversing an edge between vertices u and v. Here, the constant β_0 is the baseline kWh consumption per kilometer, upon which any coefficient is added or subtracted based on the road grade.

Lastly, to ensure connectivity and feasible solutions, a function is applied such that no edge has a traversal cost higher than the minimum battery capacity used

for this thesis' experiments; 10 kWh. Any edge with a higher cost is divided by two and an *artificial* vertex is placed between the two original vertices.

The final graph, consisting of 18 183 vertices and 26 324 edges, is illustrated below in Figure 3.3, which also includes the vertex elevation. Notice the systematically placed vertices in between long distances. While not **fully** representative of the real road network, these vertices guarantee connectivity of the reachability graphs constructed in Section 2.4 and thus feasible solutions.

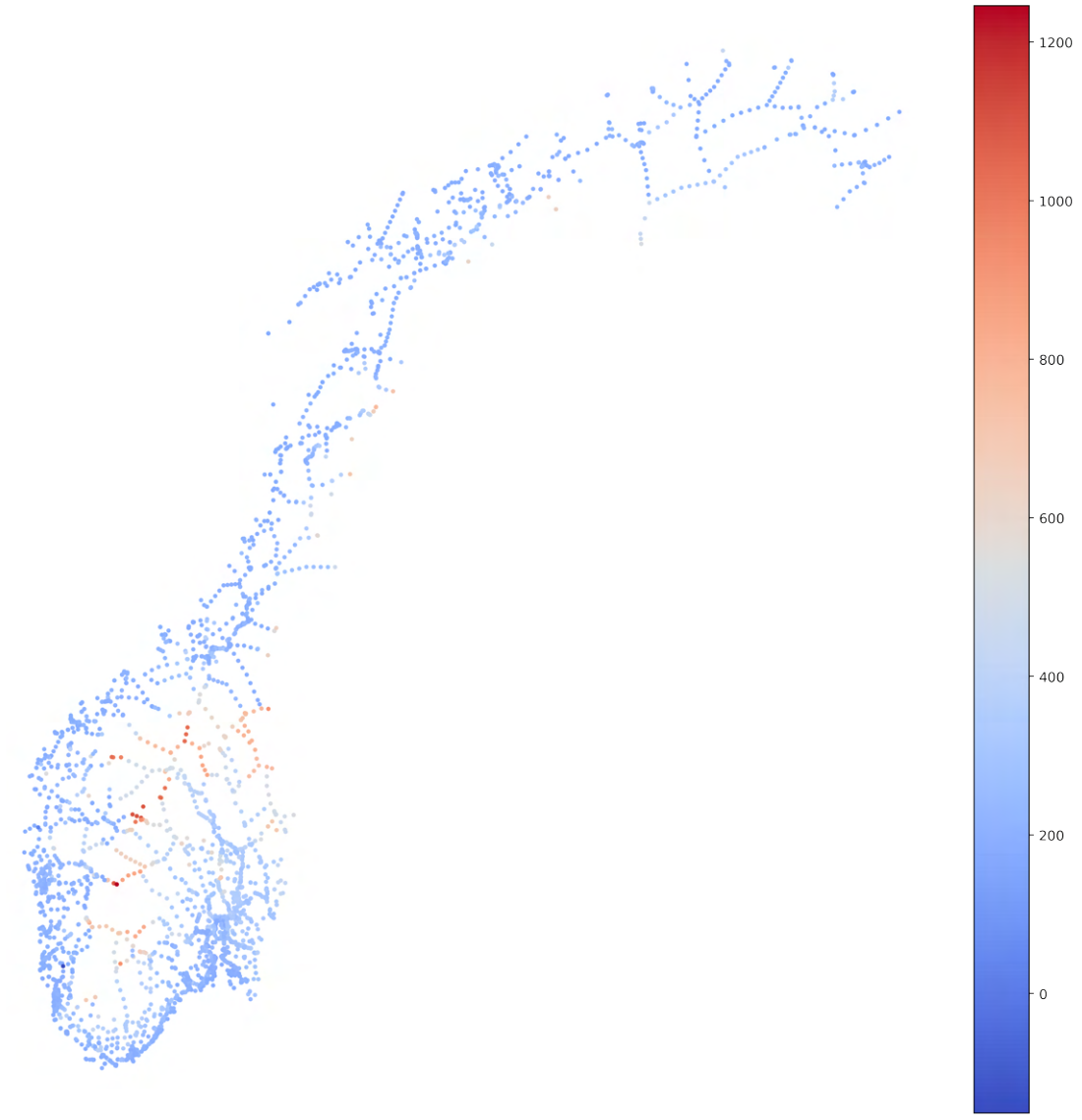

Figure 3.3: Road network for Norway, functional road class 0-3 with elevation

Due to simplification, the average vertex degree is near 3. This is expected, as most vertices in the graph are either endpoints, crossroads, or artificial vertices. The maximum degree is 5, which corresponds to the number of connections in a larger roundabout. Naturally, the minimum degree is 1, which represents the endpoints. The density of the graphs, meaning the number of *existing edges* relative to the *potential edges*, is very low. This is consistent with the graph density of other researchers (Gagarin & Corcoran, 2018; He et al., 2019; Funke et al., 2015).

Statistic	Value
Vertices	18 183
Edges	26 324
Network density	0.0002
Maximum degree	5
Average degree	2.8955

Table 3.2: Summary statistic of graph

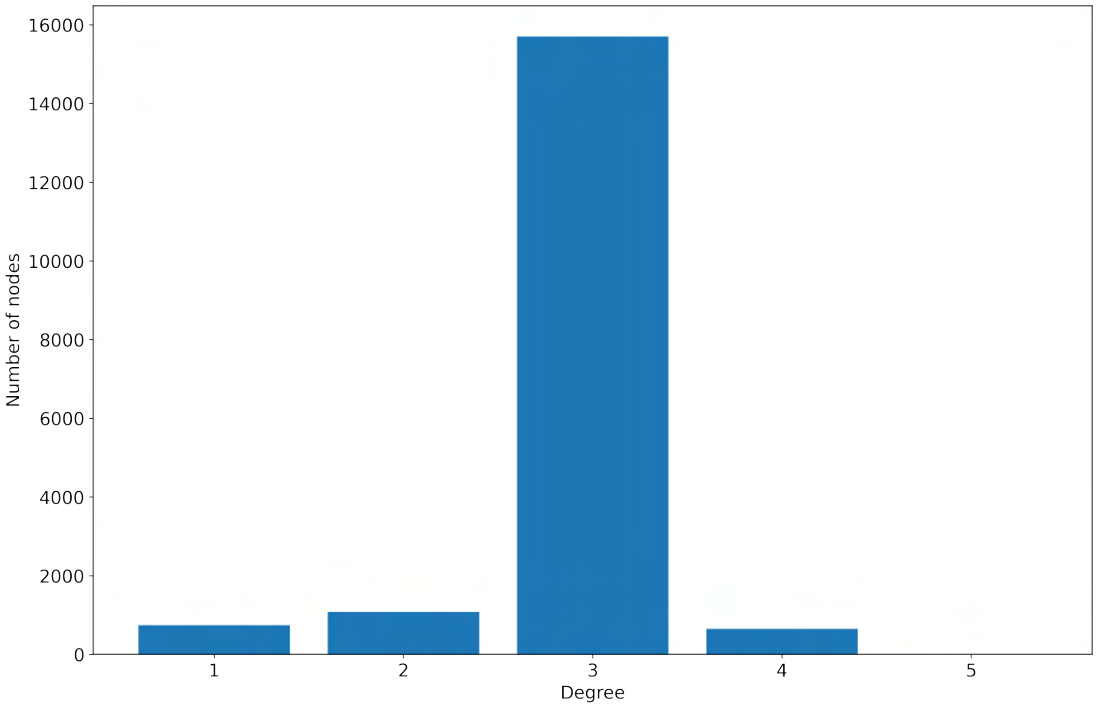

Figure 3.4: Degree distribution

4 Optimization Model

This section presents the optimization procedure for finding charging station locations, given a set of different parameters. First, it presents the current system in the context of the data created in Section 3.2.1. Secondly, it presents the concept of a *reachability graph*. Lastly, the criteria and methodologies for determining a k-dominating set and connected k-dominating set are explained.

The first step is to construct a reachability graph denoting the reachable vertices from a vertex $v \in V(G)$ using Algorithm 4.1 and 4.2. As such, the reachability graph is derived from the original graph, but all edges are computed based on a certain reachability threshold between vertices. The details of this process are explained further in Section 4.2. In short, any vertices that are reachable within the travel cost t of each other are connected by an edge. If the travel cost is greater than t, no edges between these vertices exist.

The second step is to find the locations of the charging stations using the reachability graph constructed in Section 4.2. Using a reachability graph and a **k-dominating set**, Corcoran and Gagarin (2018) allocated charging stations such that any non- charging station vertex is within a specific range of at least k charging stations. However, the structure of the k-dominating set does not guarantee that the dominating vertices are adjacent to each other. In this case, it does not guarantee that charging stations will be within the range of each other, which is a problem when addressing the issue of reachability. These issues are addressed in Section 4.3.1 and 4.3.2.

4.1 Current System

As of spring 2021, according to OpenChargeMap, the world's largest registry for electric vehicle charging stations, there exist 810 fast charging stations in 461 different locations in the graph. Tesla and other proprietary stations are

not considered in this paper, as it is not possible for non-Teslas to charge their batteries using these.

Most of these charging stations are concentrated around urban areas like Oslo-area, Kristiansand, Stavanger, Bergen, and Trondheim. To analyze and compare the current system and the proposed solutions, the current charging stations have to be interpolated into the network constructed in Section 3.2.1.

To do so, the coordinate of each existing charging station is retrieved and inserted into the nearest node on the graph using the Euclidean distance:

$$d(x, y) = \sqrt{(x_v - x_j)^2 + (y_v - y_j)^2} \tag{4.1}$$

Where x represents the longitudinal coordinate, and y is the latitudinal coordinate value, v a vertex in the graph, and j is the currently existing charging station.

Arguably, this method of calculating the nearest nodes and interpolating the existing charging station may lead to some inaccuracies. However, because most, if not all, fast charging stations are located near a road, this method is deemed sufficient for this purpose. The output of this interpolation is represented in Figure 4.1 below.

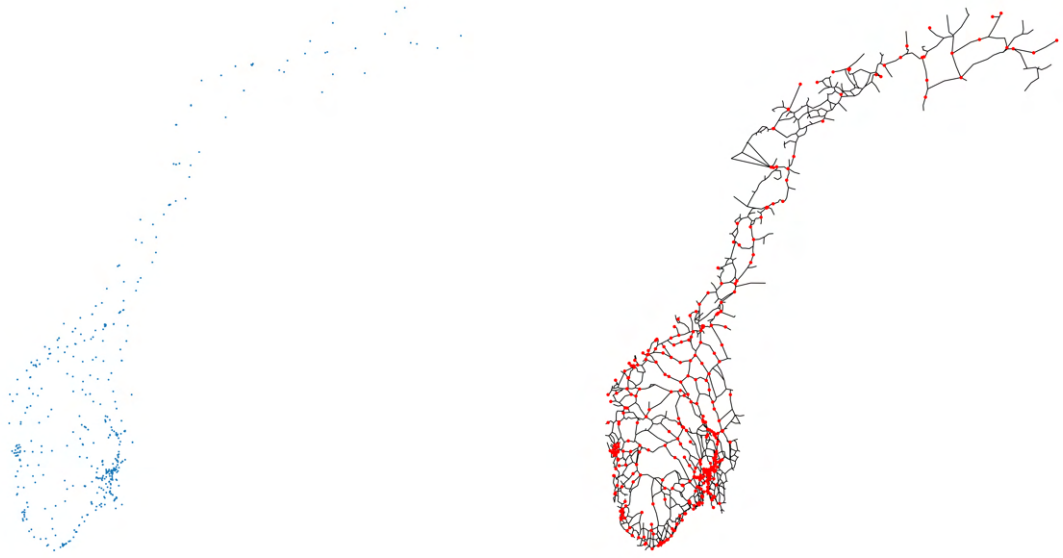

Figure 4.1: Current system (left), current system in graph (right)

At first glance, the interpolations of the current charging stations seem to accurately mimic their real location. This is the case for many of the charging stations, but there are some exceptions. When examining Table 4.1, which contains the distance in meters, the mean and median difference in distance are satisfying. However, the maximum distance is alarming. This large spread in distribution comes due to two main factors. The first is that certain islands are excluded from the graph because the ferry data is lacking. Hence, when a charging station is present on an island, its closest location in the network is often far away. Secondly, during the simplification process in Section 3.2.1 vertices with degree $\delta_v = 2$ are deleted. If a charging station is present in [or near] the deleted vertex, its location in the network would be affected by the simplification. While this is not a problem for areas with many crossroads, its effect can be significant in remote areas where the distance between the simplified edge and the next crossroad is large. Nonetheless, as this is mainly for exploration purposes and because the large distance differences are outliers, these findings do not affect the outcome of the research.

Mean dist.	Median dist.	Min dist.	Max dist.
1 493.053	248.628	16.989	37 480.049

Table 4.1: Distance difference (meters) between estimated and real locations

The considered battery capacities for this thesis are 20, 30, and 40 kWh, and a simple Dijkstra search across the currently existing charging stations shows that many charging stations are out of range for multiple vertices for all ranges. In the current system, if one is to have a charging station within range, for all locations, the required capacity would be 98.81 kWh. This capacity is equivalent to the battery capacity of a Tesla Model S, which in 2021 costs around 700 000 NOK.

Table 4.2 shows that, on average, a battery capacity of 20 kWh should be sufficient. However, the mean capacity to the nearest charging station is lowered by the skewed distribution of charging stations. Moreover, because vertices are not

uniformly distributed across the network, meaning that urban areas have more vertices than remote areas, this metric is not necessarily representative of the true state of the system.

Mean cap.	Median cap.	Min cap.	Max cap.	Std.dev	Unit
4.035	1.308	0.0002	98.811	7.3	kWh

Table 4.2: Battery consumption (kWh) from nearest charging station

Although there are many fast charging locations, the distribution of these are not adequate to satisfy full reachability across the road network. The current system requires that one owns an electric vehicle with a battery capacity of 98.81 kWh, given the estimates used in this thesis, to strictly satisfy reachability. This requirement can contribute to a slower adoption rate of electric vehicles, and thus a slower electrification of the transportation sector, as the barrier to entry costs for a feasible electric vehicle increases. Additionally, the battery consumption travel cost to charging stations is right- skewed, as presented in Figure 4.2. One reason for this is due to the sparsity of the charging stations in non- urban areas of Norway, such as the northern or western districts.

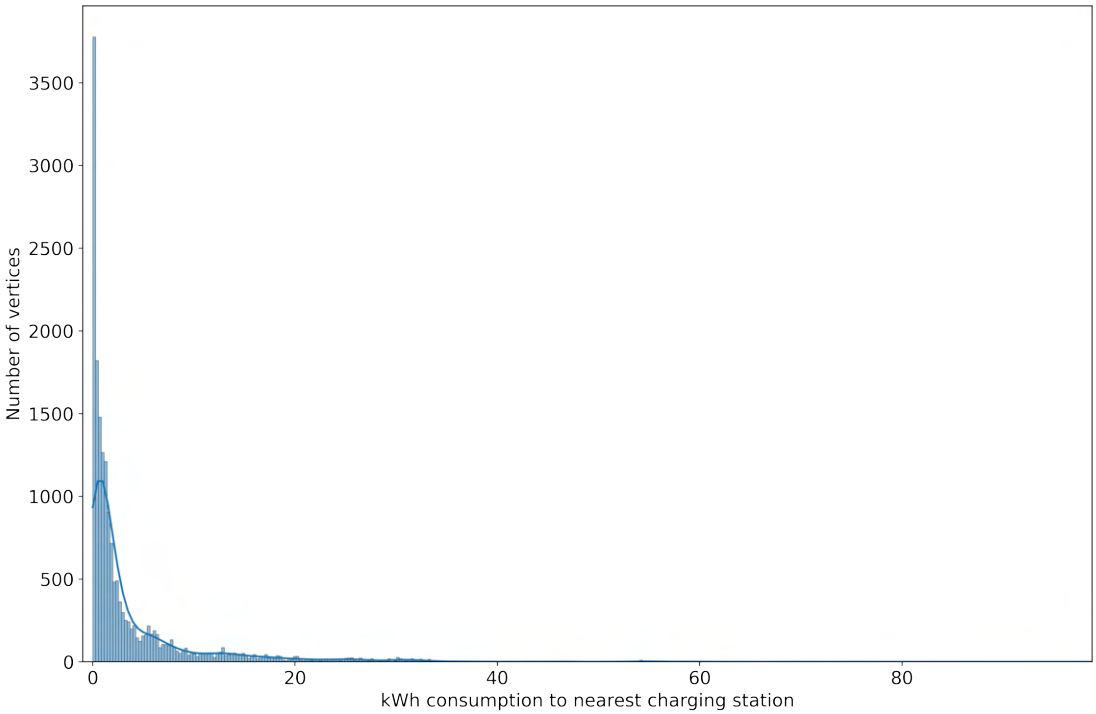

Figure 4.2: distribution of kWh consumption to nearest charging station

The findings from Table 4.2 and Figure 4.2 are illustrated in Figure 4.3 below. This figure illustrates the battery cost in kWh to the nearest charging station for all vertices in the graph. Green vertices are close to charging stations, while the red vertices are further away. Figure 4.3, which shows that urban areas have better coverage than non-urban areas, reinforces the idea that the remote parts of the country are less suited for the comfortable use of electric vehicles, and that a high battery capacity is required to travel without experiencing so-called *range anxiety*.

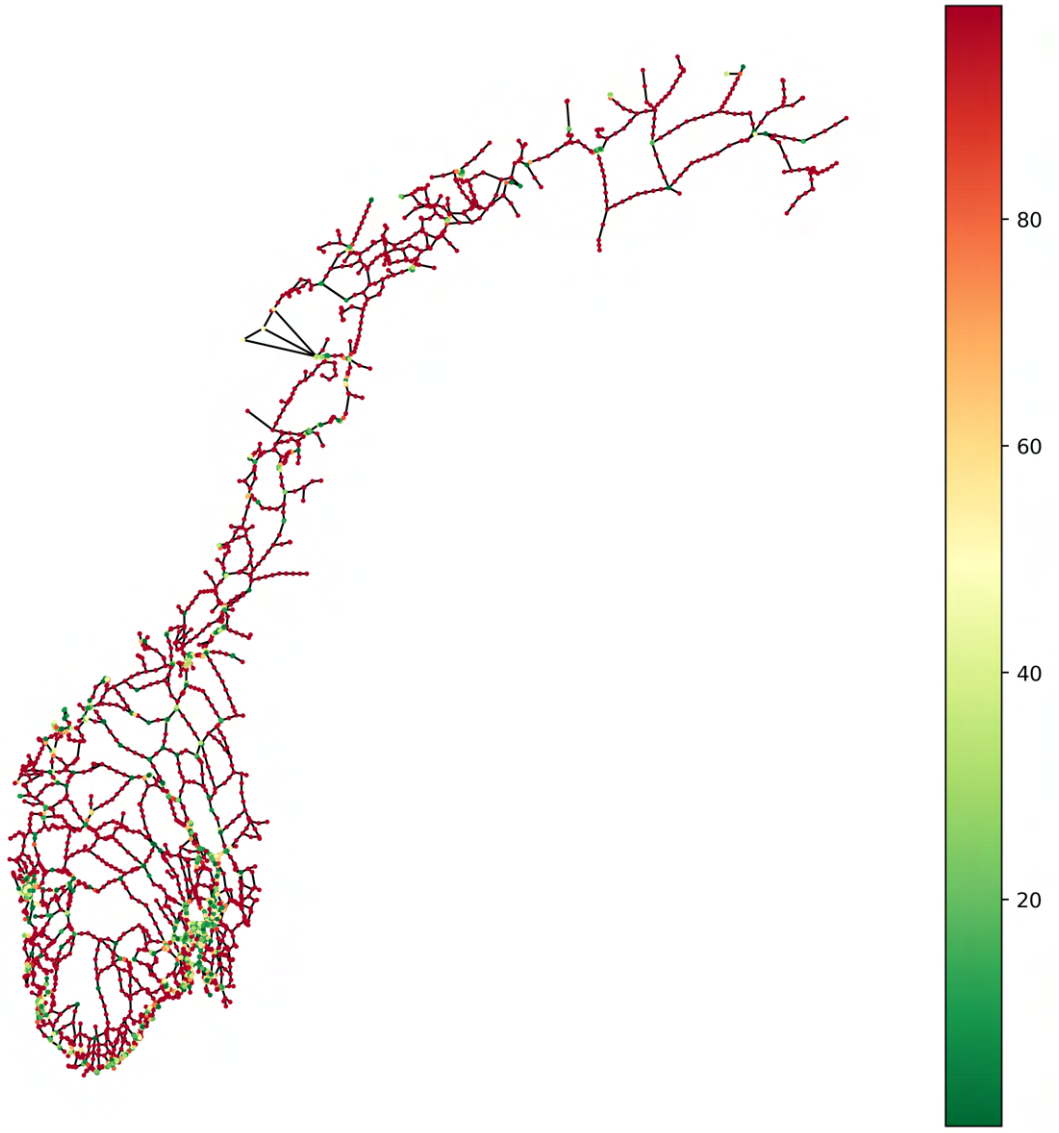

Figure 4.3: kWh cost to nearest charging station

Hence, an optimal allocation of charging stations should see that all parts of the country are covered by charging stations. This requirement is not satisfied in today's system within a *reasonable* battery capacity.

4.2 Constructing Reachability Graph

Following the steps performed by Corcoran and Gagarin (2018), a *reachability graph* G_t^r is constructed. The reachability graph represents the vertices that are reachable within a certain range of a specific vertex. Because the reachability

graph represents the weighted adjacency of each vertex, all information in the graph can be represented in a matrix:

$$G_t^r = \begin{bmatrix} g_{11} & g_{12} & g_{13} & \cdots & g_{1n} \\ g_{21} & g_{22} & g_{23} & \cdots & g_{2n} \\ g_{31} & g_{32} & g_{33} & \cdots & g_{3n} \\ \vdots & \vdots & \vdots & \ddots & \vdots \\ g_{m1} & g_{m2} & g_{m3} & \cdots & g_{mn} \end{bmatrix}$$

Where $g_{v,u}$ represents the cost of traveling from v to u if u is reachable from v within threshold t, and 0 otherwise. A neighborhood of a vertex in G_t^r is illustrated in Figure 4.4 below, where each edge represents any available vertex within 20 kWh range.

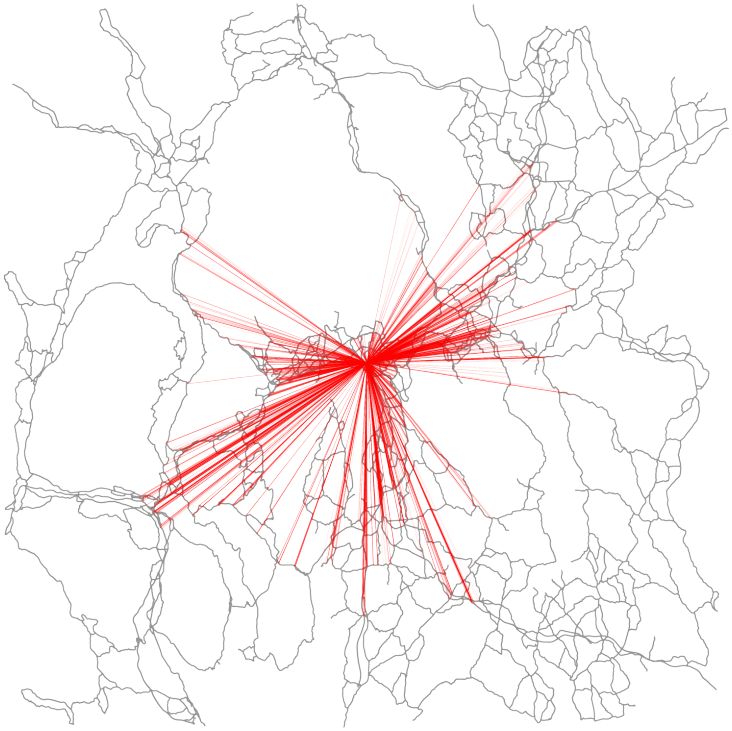

Figure 4.4: Neighborhood of vertex in reachability graph with cutoff = 20 kWh, from vertex in center of Oslo

A neighborhood of a vertex in the reachability graph is constructed using Algorithm 4.1, a modified Dijkstra's algorithm with a cutoff value, where all paths

originating from the source vertex are explored, and its vertices stored until a specific threshold is reached. As the graph is undirected, meaning that all edges are bidirectional, there is no edge traversal cost stored in the graph. The reason for this is that elevation data is included, the traversal cost must incorporate in which direction the edge is traversed. To do this, Algorithm 4.1 iteratively calculates the traversal cost for the neighborhood $N(v)$ of v. The algorithm first evaluates the elevation difference between $u \in N(v)$ and v. Subsequently, the edge gradient and associated battery consumption were calculated using the values from Table 3.1.

Lines 1-2 define the input and output of the procedure. Line 3 instantiates Q, which is the set of all vertices in G. Lines 4-6 assigns infinite travel cost to all vertices, except for the source vertex which is assigned a cost equal to 0. Line 7 instantiates the array *visited* which contains all visited vertices. Lines 8-25 is repeated as long as there are vertices in Q. In each iteration, line 9 assigns u as *None* and the cost to u as infinite. Line 10-14 iterates through the vertices in Q, checks if it the new path is less costly than the current path and assigns a new u. Lines 15-16 return the *cost* array, where the cost is less or equal to t, so that vertices where the cost is infinity are discarded. Line 17-18 adds u into *visited* and removes u from Q. Lines 19-25 computes the cost between u and its neighbors $n \in N(u)$ based on the elevation differences, and defines c as travel cost between u and n. If the travel cost is higher or equal than the threshold, disregard the path, otherwise update *cost*.

Algorithm 4.1 Dijkstra with cutoff threshold

1: **Input:** A Graph G^s, a *source* $\in (G^s)$, a threshold $t \in \mathbb{R}$
2: **Output:** Set of vertices within range t of source
3: $Q \leftarrow V(G^s)$
4: **for** *each* $v \in Q$ **do**
5: $cost_v := \infty$ // $cost_v$ is the kWh cost of visiting v from *source*
6: $cost_{source} := 0$
7: visited $= \emptyset$
8: **while** Q $\neq \emptyset$ **do**
9: $u = None$
10: $cost_u := \infty$
11: **for** v in Q **do**
12: **if** $cost_v < cost_u$ **then**
13: $cost_u := cost_v$
14: $u := v$
15: **if** $u = None$ **then** // When no condition is satisfied
16: **return** $cost : cost_v < t \quad \forall \quad v \in V(G^s)$ // Return only vertices within threshold t
17: visited $\leftarrow u$
18: $Q := Q \setminus u$
19: **for** each $n \in N(u)$ **do**
20: $c_{u,n} :=$ *kWh cost based on vertex elevation difference and length*
21: $c := c_{u,n} + cost_u$ // c is cost to neighbor plus accumulated cost
22: **if** $c > t$ **then** // If c surpasses threshold, check next neighbor
23: **continue**
24: **if** $c \leq cost_n$ **then**
25: $cost_n := c$

The reachability graph is constructed by running Algorithm 4.1 on each vertex, and constructing edges with the edge weight as the battery cost in each direction. This process also implies that the graph is converted to a directed graph, meaning that the graph now considers the direction of the edges and that edges e_{uv} and e_{vu} may inflict different traversal costs. This procedure is presented in Algorithm 4.2.

Line 3 creates an empty matrix A^t. Lines 4-8 iterate through all vertices, compute

the reachable vertices from the vertex u within threshold t using Algorithm 4.1. In line 6, a vector B_v^t with dimensions $1 * |V(G)|$ is constructed, which contains the travel cost between u and v if they are in the range of each other, otherwise the value is zero. In line 7, the corresponding vector in A^t, namely A_v^t, is updated and replaced by B_v^t. Line 8 returns the new adjacency matrix A^t.

Algorithm 4.2 Full reachability graph construction

1: **Input:** A graph G, a kWh threshold t

2: **Output:** A full reachability graph adjacency matrix A^t

3: Let A^t denote a null matrix with dimensions $|V(G)| * |V(G)|$

4: **for** each $v \in V(G)$ **do**

5: $costs_v^t = Dijkstra\ with\ cutoff\ threshold(v, t)$

6: Create a vector B_v^t denoting the reachable neighborhood of v such that:

$$B_{v,u}^t = \begin{cases} costs_v^t[u], & \text{if } u \text{ is reachable from } v \\ 0, & \text{otherwise} \end{cases}$$

7: $A_v^t := B_v^t$ // Replace empty values of A_v^t with B_v^t

8: **return** A^t // Return the adjacency matrix for G_t^r

Algorithm 4.2 is repeated five times. One for each range of 10, 15, 20, 30, and 40 kWh, such that one graph for each range is constructed.

One feature of Algorithm 4.2 is that it constructs a directed graph with parallel edges. This means that the travel cost from v to u can be 1 kWh, but the travel cost from u to v can be 0.7 kWh because of differences in elevation. This property implies that certain vertices are connected one way, but not the other. Therefore, due to constraints of the *connected k-dominating set* explained in Section 4.3.2, the graph is converted to an undirected graph in which the highest of the two edge costs are considered. Additionally, if an edge only exists in one direction, the undirected graph considers that edge to be non- existent. In other words; only the worst travel cost is considered.

For the reachability graphs of 10 and 15 kWh, the minimum vertex degree is 0. This is because with such a low reachability threshold, certain vertices become isolated as no other vertex is reachable. In these cases, a *connected k-dominating set* cannot be constructed, because it violates the constraints for connectivity. However, because these graphs are to be applied for range threshold double of their respective reachability value, e.g. 20 kWh for G^r_{10} and 30 kWh for G^r_{15}, the vertices can still be available for use in k-dominating sets, even though the vertex is disconnected in the reachability graph. Metrics for each reachability graph are presented in Table 4.3.

kWh	Edges	Mean degree	Min degree	Max degree	Density
10	7 758 978	426.716	0	1 883	0.047
15	12 065 776	663.575	0	2 358	0.073
20	16 927 686	930.962	1	3 074	0.102
30	28 776 480	1 582.604	3	4 801	0.174
40	41 709 348	2 293.865	6	6 020	0.252

Table 4.3: Reachability graphs characteristics

The connectivity of the graphs increases as the kWh reachability threshold increases from 10 to 40 kWh, which is also observable in Figure 4.5 below. The higher the range, the more vertices are reachable from any given vertex, and the more edges are added to the graph. Hence, increasing the kWh range strictly increases the degrees of the vertices and increases the density of the graph. This effect is illustrated in Figure 4.5, which plots the estimated distribution density of the degrees for each reachability graph. The figure shows that when the reachability threshold increases, then the distribution becomes less skewed and flattens; compare, for instance, the distribution of 10 kWh which is left skewed, while 40 kWh follows a more uniform distribution.

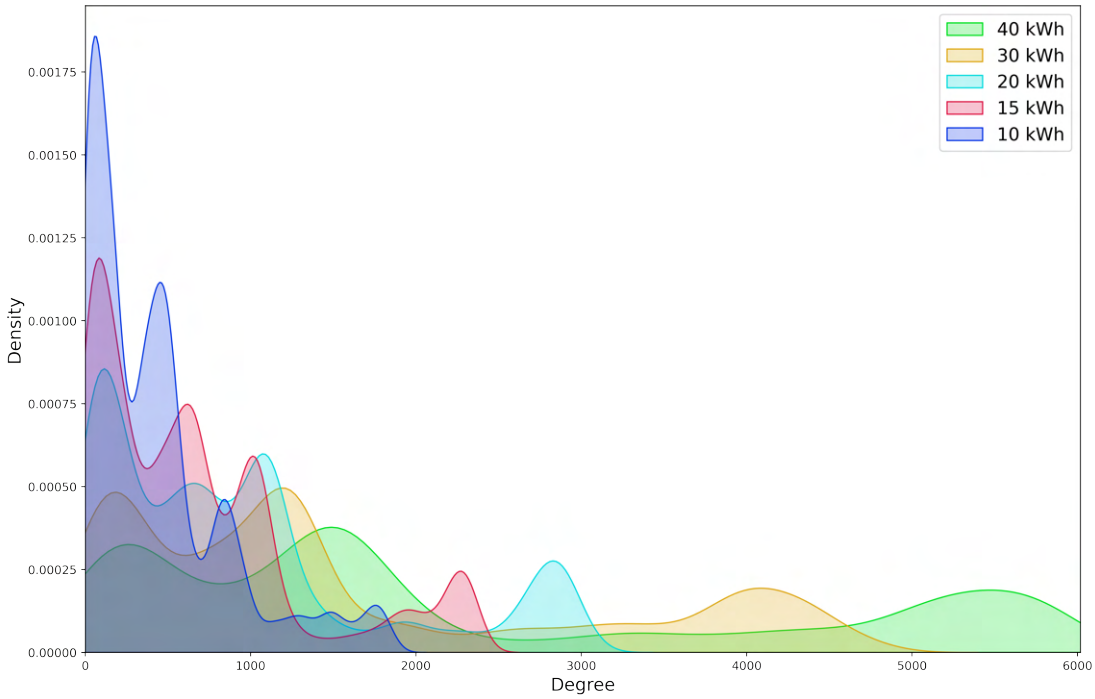

Figure 4.5: Degree distribution of reachability graph

There are several issues with the size of the reachability graph. Firstly, the size of the graph represents a challenge when loading the graph into memory. This problem can be partly solved by loading the graph as a sparse adjacency matrix rather than a graph object. This is done using the *SciPy* package in Python. Secondly, performing computations on graphs of these sizes can be time-consuming. This issue is addressed in the next chapter.

4.3 Vertex Domination

To satisfy the constraint that every non-charging station vertex is at most t kWh units away from a charging station, one can construct a *dominating set* using the reachability graphs. A dominating set is a set $D \subseteq V(G)$ such that every vertex $v \in V(G) \setminus D$ is adjacent to **at least one** vertex in D. However, in the case of this experiment, a dominating set is susceptible to large shortest path deviations recuding the adoption of electric vehicles. Therefore, a *k-dominating set* can be constructed. A k-dominating set, first coined by Flink and Jacobson

in 1985 (Fink & Jacobson, 1985; Bakhshesh, Farshi, & Hasheminezhad, 2017), is similar to a dominating set, except that each vertex $v \in V(G_r^t) \setminus D$ must be adjacent to **at least** k vertices in D. This means that a set D is k-dominating if $|\{v \in V(G_r^t) \setminus D \colon |N(v) \cap D| < k\}| = 0$ (Gagarin & Corcoran, 2018). Where $N(v)$ represents the neighbors of vertex v, and k is the number of required neighbors in D.

One weakness with the k-dominating set (and dominating set), for this application, is that it does not guarantee that vertices in the dominating set are adjacent to each other. Hence, charging stations are not guaranteed to be within the range of each other. For instance, consider the graph presented in Figure 4.6, which is dominated ($k = 1$) by red nodes. If each edge represents one battery capacity, one can not successfully travel from vertex 2 to vertex 3, 6, 5, and 9.

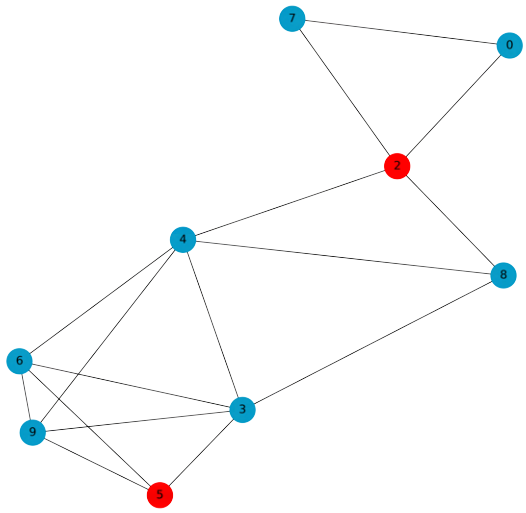

Figure 4.6: 1-dominating set

This thesis employs two methods for optimally allocating charging stations. The first is using the discussed k-dominating set, which might include isolated charging stations. Secondly, a *connected k-dominating set (CkDS)* can be constructed. This solves all problems in the k-dominating set, but the cardinality of the solution is higher, at least for similar range thresholds. This is further elaborated in Sections 4.3.1 and 4.3.2 respectively.

4.3.1 k-Dominating Set

Given a graph $G(V, E)$, a set $D \in V(G)$ is *k-dominating* if every vertex $v \in V(G) \setminus D$ is adjacent to at least k vertices in D. The *minimal* k-dominating set $\gamma_k(G)$ can be formulated using integer linear programming:

$$\text{minimize} \sum_{v \in V(G)} x_v \tag{4.2}$$

subject to:

$$\sum_{v \in N(u)} x_v \geq (1 - x_u)k \qquad \forall \quad u \in V(G) \tag{4.3}$$

$$x_v \in \{0, 1\} \qquad \forall \quad v \in V(G) \tag{4.4}$$

Where:

- x_v is the decision variable, $x_v = 1$ if x_v is dominating
- $V(G)$ is the set of vertices in G
- $N(u)$ is the set of neighbors of a vertex u
- k is the threshold value for k-domination

The objective function (4.2) minimizes the total number of vertices present in the dominating set $D \subseteq V(G)$. Constraint (4.3) ensures that the neighborhood of each vertex, $N(v)$, contains at least k vertices where $x_v = 1$. Constraint (4.5) confines x_v to a binary variable.

Finding $\gamma_k(G)$ is known to be NP-hard. Hence, heuristics must be used for finding solutions within a reasonable time frame. Corcoran and Gagarin (2018) employ an algorithm named *randomized k-dominating set*, which is presented in Algorithm 4.3 below.

Line 3 defines δ' based on the mean vertex degree,$\overline{\delta}$, and k. Line 4 computes the probability p of a vertex being part of the dominating set. Line 5 instantiates

an empty set A. Lines 6-7 iterate through all vertices in the graph and assign vertices to A with probability p. Line 8 instantiates an empty set B. Lines 9-10 iterate through all vertices not in A and adds them into B if their neighborhood in A is less than k. Line 11 defines D as the union between A and B. Because the output of Algorithm 4.3 is not necessarily minimal, line 12 reduces the size of D by employing Algorithm 4.4.

Algorithm 4.3 Randomized k-dominating set (Gagarin and Corcoran, 2018)

1: **Input:** A reachability graph G_t^r, a number $k \in \mathbb{R}$
2: **Output:** A dominating set D
3: let $\delta' = \overline{\delta} - k + 1$
4: $p = 1 - \frac{1}{\sqrt[\delta']{b_{k-1}(1+\delta')}}$ // Calculate probability
5: $A = \emptyset$ // Instantiate empty set A
6: **for** each $v \in V(G_r^t)$ **do**
7: $A \leftarrow v$, with probability p // Put v into A with probability p
8: $B = \emptyset$ // Instantiate empty set B
9: **for** each $v \in V(G_r^t) \setminus A$ **do**
10: **if** $|N(v) \cap A| < k$ **then** $B \leftarrow v$
11: $D = A \cup B$
12: Perform *minimal k-dominating set* algorithm to reduce $|D|$
13: **Return** D // Return a k-dominating set D

Line 3 of Algorithm 4.4 below sorts the vertices in the k-dominating solution by their number of nondominating neighbors in nondecreasing order. Lines 4-5 iterate through each vertex v, checks if D is still k-dominating without v. If so, line 6 removes v from D.

Algorithm 4.4 Minimal k-dominating set (Gagarin and Corcoran, 2018)

1: **Input:** A complete reachability graph G_t^r, a dominating set $D \subseteq V(G)$
2: **Output:** A minimal k-dominating set D
3: $L = (v_1, ..., v_{|D|}) : v \in D, |N(v_i) \setminus D| \leq |N(v_{i+1}) \setminus D|$
4: **for** each $v \in L$ **do** // For each vertex ordered by neighbors not in D
5: **if** $D \setminus \{v_i\}$ *is-k-dominating* set of G_t^r **then**
6: $D = D \setminus v_i$ // $\{v_i\}$ is redundant
7: **Return** D

Line 7 checks if the set is k-dominating in the given graph, with a domination condition of k. This algorithm iterates through every vertex $v \in V(G)$ of the input graph and counts the number the vertex has in D. If a vertex has less than k neighbors in D, e.g. $|N(v) \cap D| < k$, the algorithm breaks the loop and returns $False$. Hence, when the input solution D is k-dominating, the algorithm must iterate through all vertices, which is time-consuming.

4.3.2 Connected k-Dominating Set

Given a graph $G(V, E)$, a set $D \in V(G)$ is *connected k-dominating* if every vertex $v \in V(G) \setminus D$ is adjacent to at least k vertices, and the induced subgraph from D is connected (Hansberg, 2010). The mathematical formulation of the minimal *CkDS* is very similar to the k-dominating set formulation, with one additional constraint:

$$\text{minimize} \sum_{v \in V(G)} x_v \tag{4.5}$$

subject to:

$$\sum_{v \in N(u)} x_v \geq (1 - x_u)k \qquad \forall \quad u \in V(G) \tag{4.6}$$

$$\sum_{v \in N(u)} x_v \geq x_u \qquad \forall \quad u \in V(G) \tag{4.7}$$

$$x_v \in \{0, 1\} \qquad \forall \quad v \in V(G) \tag{4.8}$$

Where:

- All variables are the same as in 4.2 to 4.4

Constraint (4.7) ensures that all nodes are connected, and thus ensures connectivity in the dominating set D. Constraint (4.5) confines x_v to a binary variable.

Finding a minimum connected k-dominating set is NP-hard (B. Liu et al., 2016). Therefore, to find a feasible solution, Algorithm 4.5 is to be used. Algorithm 4.5 is a greedy algorithm inspired by Fu et al. (2016), but adjusted to construct a *connected k-dominating set* instead of a *connected dominating set* (Fu, Han, Yang, & Jhang, 2016).

Algorithm 4.5 categorize the vertices into four different colors. White vertices are vertices that are *uncovered*, have no neighbors in the dominating set, and are not part of the dominating set. Red vertices are those that are part of the dominating set. Yellow vertices are candidate vertices, which must be adjacent to red vertices. Green vertices are covered vertices which must be adjacent to at least k red vertices.

Line 3 instantiates an empty set *colors*. Lines 4-5 assign all vertices in *colors* as *white*. Line 6-7 selects the vertex in $V(G)$ with the highest degree, and colors it *red*. Lines 8-9 assigns all neighbors of v as candidate vertices, and therefore

the color *yellow*. Lines 10-24 are repeated until a connected k-dominating set is found. Lines 11-13 check if any remaining vertices are yellow and adjacent to only green and red vertices. If so, all remaining vertices are colored red, as they must be part of the connected k-dominating set. Lines 14-15 select the yellow vertex with most yellow and white neighbors, and color it red. Lines 16-20 iterate through the neighbors of the latest red vertex and color them yellow if the vertex was previously white, or green if it has at least k red neighbors. Lines 21-24 create an empty set D and inserts it all the red vertices from $colors$.

Algorithm 4.5 Greedy connected k-dominating set, G-CkDS

1: **Input:** A graph G, an integer $k \geq 1$
2: **Output:** A connected k-dominating set
3: $color = \emptyset$ // Instantiate empty set of colors
4: **for** each $v \in V(G)$ **do**
5: $color_v := white$
6: select $v \in V(G)$ with the highest degree
7: $color_v := red$ // Color v red (dominating)
8: **for** each $u \in N(v)$ **do**
9: $color_u := yellow$ // Set each neighbor of v as candidate vertex
10: **while** any *white* or *yellow* vertices exists **do**
11: **if** remaining vertices are *yellow* and adjacent to only *green* and *red* vertices **then**
12: color remaining vertices *red*
13: **break** // Break while-loop
14: select *yellow* vertex $v \in V(G)$, with most *yellow* and *white* neighbors.
15: $color_v := red$ // Color v red
16: **for** each $u \in N(v)$ **do**
17: **if** $color_u = white$ **then** // If $color_u$ is white
18: $color_u := yellow$ // Set $color_u$ yellow
19: **if** u has at least k *red* neighbors **then**
20: $color_u := green$ // u is k-dominated, color u green
21: $D = \emptyset$ // Instantiate empty dominating set D
22: **for** each $v \in V(G)$ **do** // Put all red vertices in D
23: **if** $colors_v = red$ **then**
24: $D \leftarrow v$
25: **Return** D // Return CkDS

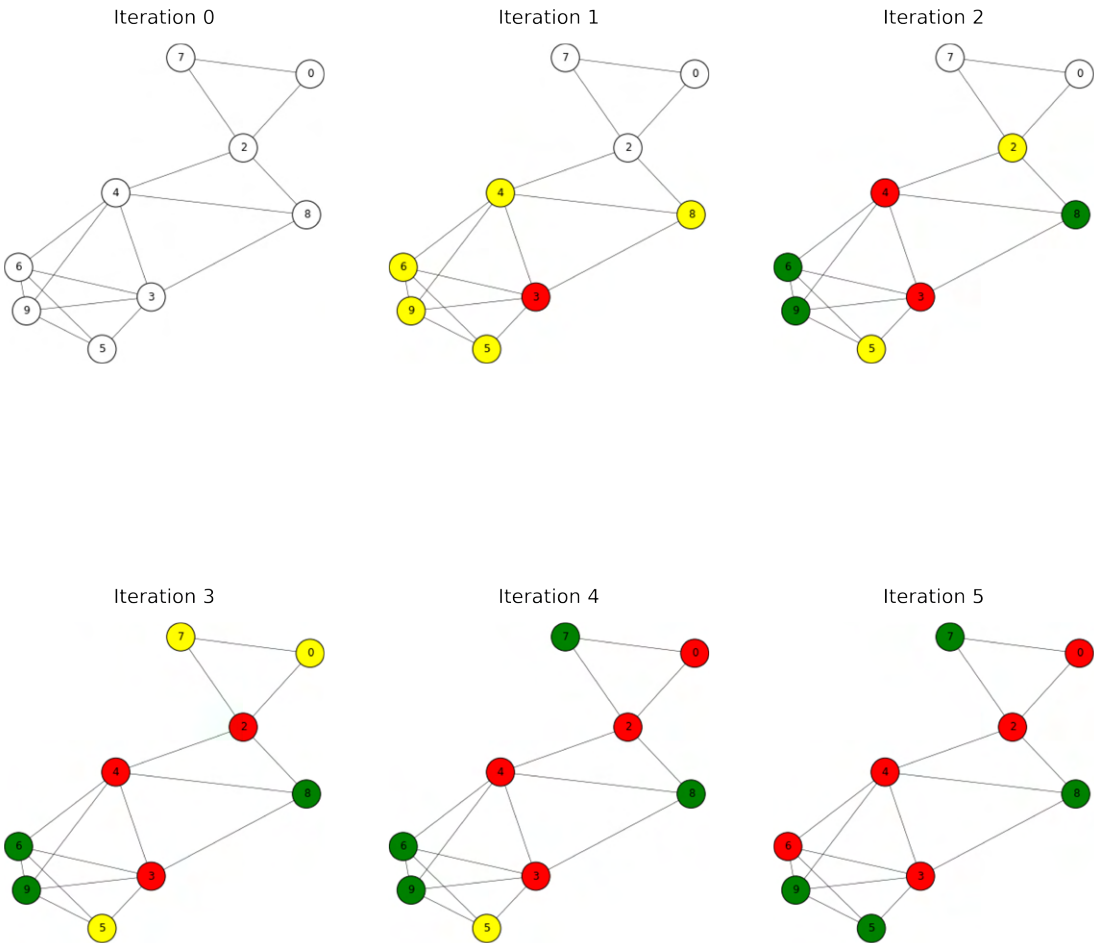

Figure 4.7: G-CkDS iteration, k = 2

An example of an execution of the *G-CkDS* is shown in Figure 4.7, with k = 2. In iteration 0, the graph is instantiated. Then, vertex 3 is colored red because it has the highest degree and lowest index value. Then, all of 3's neighbors are colored yellow. Among the yellow vertices, vertex 4 is now colored red, and its non- yellow neighbors colored yellow. Because vertices 6 and 9 are both adjacent to at least two red vertices (3 and 4), they are colored green. This process is repeated until iteration 5, when vertex 6 is colored red because it is adjacent to yellow vertex 5. The dominating set is in this case also a minimum cardinality connected k-dominating set, $\gamma_2(G)$. However, it is worth noting that the *G-CkDS* does **not** guarantee for an optimal solution, but only a [greedy] feasible one.

Algorithm 4.6 Prune greedy connected k-dominating set, PGCkDS

1: **Input:** A graph G, a set D, an integer $k \geq 1$
2: **Output:** A pruned connected k-dominating set
3: Sort vertices in D in ascending order of degree
4: **for** each $v \in D$ **do**
5: **if** $D \setminus v$ is connected k-dominating set **then**
6: $D = D \setminus v$
7: **Return** D

To improve the greedy solution by reducing its cardinality, Algorithm 4.6 is applied. Algorithm 4.6 prunes the solution by iterating through each vertex $v \in D$ and checking if $D \setminus v$ is still a connected k-dominating set. If so, then the vertex v is removed from the dominating set D.

5 Results

This section presents the findings from both the k-dominating set and connected k-dominating set algorithms, and compares a sample of the two variations. For the sake of this thesis, a dominating set is found for each reachability graph, with k ranging from 1 to 4, meaning a total of 12 sets for each variation. Algorithms are executed on a computer with 16 GB of RAM and a Ryzen 5 3600 - 3.6 GHz CPU.

5.1 k-Dominating Set

Computing 12 k-dominating sets took 10.5 hours in total, with an average computation time of 49 minutes per set. Higher values of k and range would lead to higher computation time. The reason for the high computation time is due to the reduction in the cardinality of the sets, performed by Algorithm 4.4.

Table 5.1 below shows the kWh distance metrics for each proposed solution. Not surprisingly, the sets are strictly decreasing with range and increasing with k.

(range, k)	Mean dist.	Median dist.	Min dist.	$\|D\|$
(10, 1)	5.449	5.781	0.0014	531
(10, 2)	5.323	5.588	0.0014	914
(10, 3)	5.348	5.604	0.0009	1293
(10, 4)	5.394	5.722	0.0009	1589
(15, 1)	8.449	9.084	0.0015	340
(15, 2)	8.179	8.637	0.0013	621
(15, 3)	8.215	8.820	0.0013	861
(15, 4)	8.127	8.574	0.0013	1084
(20, 1)	10.922	11.476	0.0020	237
(20, 2)	11.167	11.657	0.0016	443
(20, 3)	11.213	11.904	0.0015	635
(20, 4)	10.786	11.233	0.0011	807

Table 5.1: kDS: kWh distances to charging stations for proposed solutions

Metrics for the number of neighbors for nodes not in the k-dominating sets, $|N(v) \cap D|$, are presented in Table 5.2 below.

(range, k)	Mean nbrs.	Median nbrs.	St.dev.	Max nbrs.
(10 [20], 1)	5.870	6	2.246	12
(10 [20], 2)	10.358	10	3.565	20
(10 [20], 3)	14.996	14	4.974	30
(10 [20], 4)	19.783	19	6.512	36
(15 [30], 1)	6.977	6	2.656	14
(15 [30], 2)	12.472	12	3.587	21
(15 [30], 3)	18.455	18	5.723	33
(15 [30], 4)	23.819	23	7.333	41
(20 [40], 1)	6.992	7	2.359	12
(20 [40], 2)	13.262	13	3.366	21
(20 [40], 3)	19.332	19	5.250	34
(20 [40], 4)	26.146	26	7.372	42

Table 5.2: kDS: Number of charging stations within range of each vertex

As observable in Figure 5.1 below, the relationship between the range and solution cardinality is seemingly negatively non- linear. Consider, for instance, $k = 2$, whereas the range increases, the solution size decreases logarithmically. Conversely, the data suggests a linear relationship within each range as k increases.

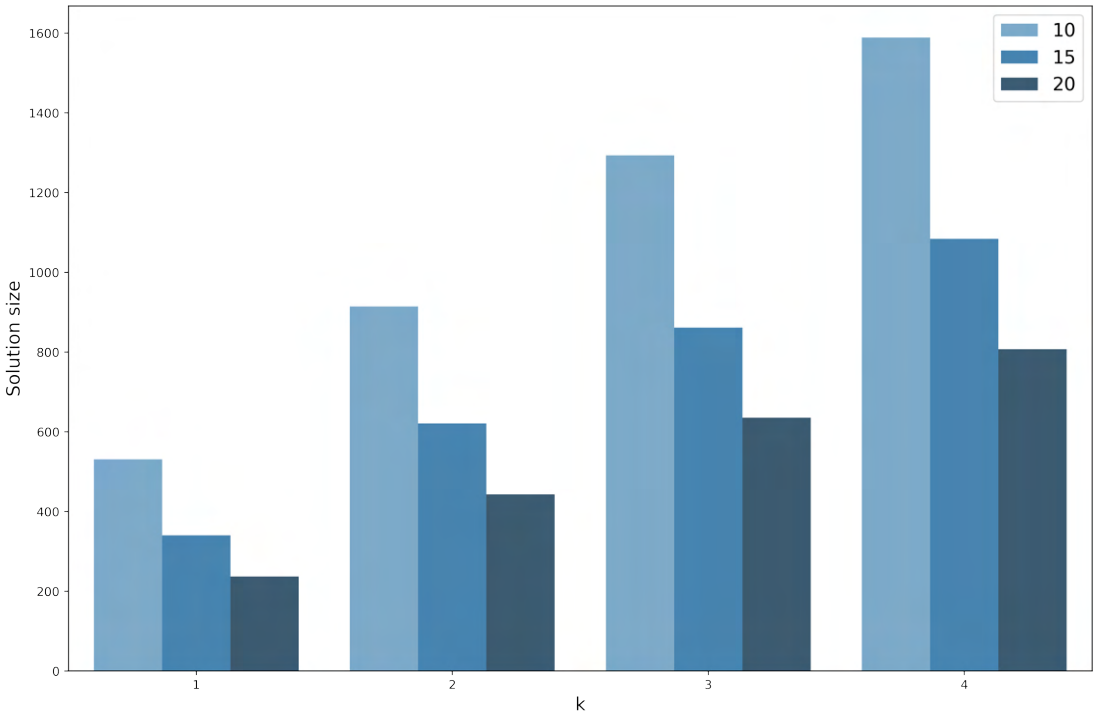

Figure 5.1: kDS: solution size and k by range

5.2 Connected k-Dominating Set

Computing 12 connected k-dominating sets took 12.6 hours in total (without pruning), with an average computation time of 62 minutes. In this case, the algorithm is severely slowed down by line 12 of the G-CkDS, where the yellow vertex with most yellow and white neighbors is selected. Higher values of k and range would generally lead to higher computation time. However, the computation time across k for each range was very similar.

The mean, median, minimum, and maximum kWh distances for each $v \in V(G) \setminus D$ are presented in Table 5.3. Naturally, the higher the range, the lower the required number of charging stations. Conversely, the higher value of k, the higher the number of required charging stations. Minimum distance is very low due to vertices in high-density clusters in the graph, which allows for the vertices being extremely close to charging stations. On the other hand, the maximum distance is always equal to the range requirement.

On average, Algorithm 4.6 reduced the cardinality of each set by 7%, with larger reductions on higher values of k, and smaller reductions on higher ranges. This is presented in columns $|D_1|$ and $|D_2|$.

(range, k)	Mean dist.	Median dist.	Min dist.	$\|D\|_1$	$\|D\|_2$
(20, 1)	11.691	12.447	0.0030	300	296
(20, 2)	11.526	12.316	0.0022	473	445
(20, 3)	11.538	12.242	0.0019	670	614
(20, 4)	11.558	12.283	0.0016	883	804
(30, 1)	18.270	19.737	0.0024	160	157
(30, 2)	18.272	20.092	0.0024	258	242
(30, 3)	18.427	20.228	0.0024	385	347
(30, 4)	18.344	20.226	0.0022	509	455
(40, 1)	24.563	26.106	0.0026	99	99
(40, 2)	24.637	26.804	0.0024	164	151
(40, 3)	25.067	27.430	0.0010	245	218
(40, 4)	24.842	27.174	0.0010	328	293

Table 5.3: CkDS: kWh distances to charging stations for proposed solutions

Additionally, some metrics for the charging stations within range, $|N(v) \cap D|$, are computed for each $v \in V(G) \setminus D$. These characteristics are presented in Table 5.4. As expected, the mean number of available charging stations within the range of each vertex increases as k increases.

(range, k)	Mean nbrs.	Median nbrs.	St.dev.	Max nbrs.
(20, 1)	2.949	3	0.978	6
(20, 2)	4.354	4	1.321	9
(20, 3)	6.038	6	1.901	13
(20, 4)	8.147	8	2.627	17
(30, 1)	3.079	3	1.058	6
(30, 2)	4.562	4	1.520	9
(30, 3)	6.800	6	2.199	15
(30, 4)	8.726	8	2.678	18
(40, 1)	3.353	3	1.208	7
(40, 2)	4.512	4	1.607	11
(40, 3)	6.391	6	2.317	15
(40, 4)	8.768	8	3.263	20

Table 5.4: CkDS: Number of charging stations within range of each vertex

Figure 5.2 below suggests a non- linear relationship between changes in range and solution size for the computed values. The cardinality of the *CkDS* is seemingly decreasing more rapidly than that of the k-dominating set.

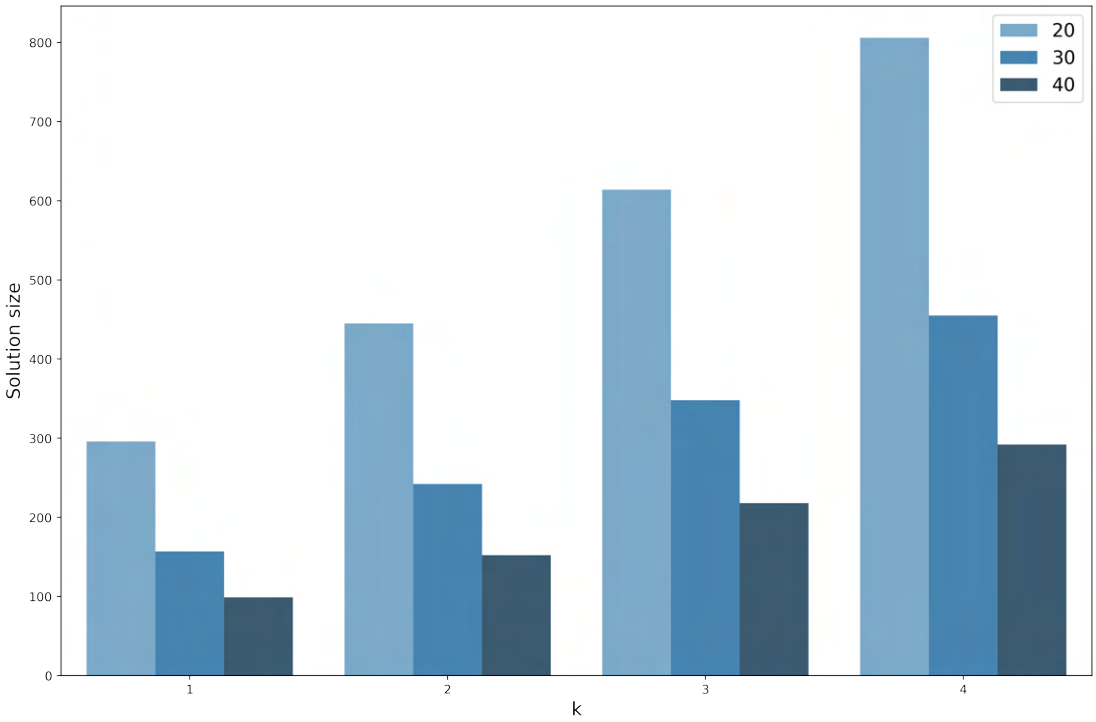

Figure 5.2: CkDS: solution size and k by range

5.3 Comparison

Due to the reachability graph threshold, the connected k-dominating sets had much lower cardinality than the k-dominating sets. Both the k-dominating set and the connected k-dominating set guarantee for reachability across the entire network. However, while the connected k-dominating set does not guarantee for round-trip reachability, the k-dominating set with half-range reachability graphs does guarantee for drivers to be able to drive back and forth between locations. Yet, this thesis assumes that drivers can charge at the target location and that reachability is satisfied with one-way trips. For instance, consider the (10, 2) and (20, 2) *kDS* and *CkDS* respectively. Both these sets try to satisfy full reachability across the road network for EVs with 20 kWh battery capacity. The kDS solution has 914 vertices, while the CkDS has 445. However, as presented in Table 5.5 below, the k-dominating set with half-range reachability graphs allocates too many charging stations, as there are on average more than twice the amount of adjacent

charging stations present for each vertex.

(Range, k)	Mean nbrs.	Median nbrs.	St.dev.	Max nbrs.
(10, 2) kDS	10.358	10	3.565	20
(20, 2) CkDS	4.364	4	1.324	9

Table 5.5: Comparison of neighbors in $kDS_{10,2}$ and $CkDS_{20,2}$

Both dominating sets are represented in Figure 5.3 below, where the dominating vertices are represented as red. The difference in cardinality between both solutions is clearly represented here.

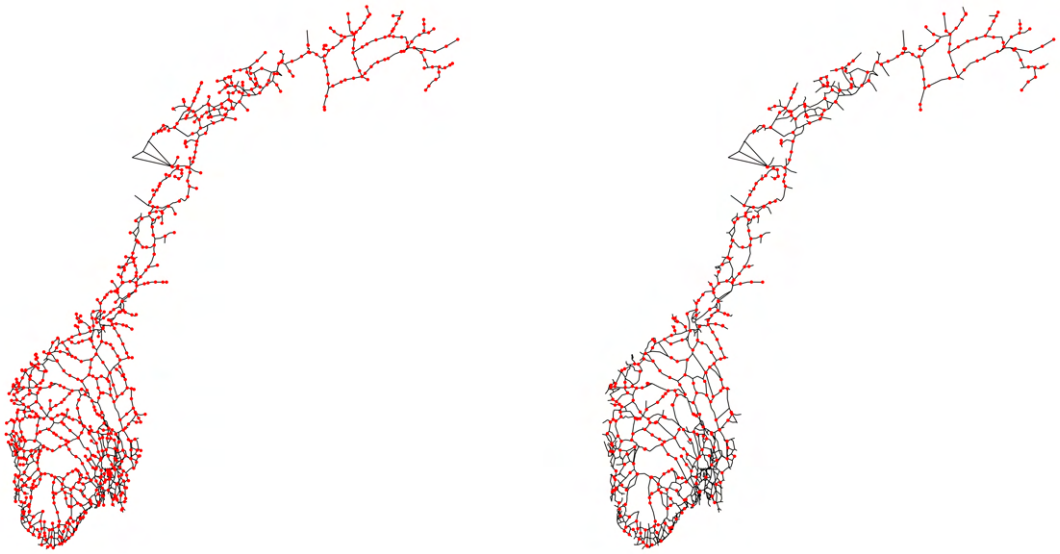

Figure 5.3: $kDS_{10,2}$ (left) and $CkDS_{20,2}$ (right)

The findings from these experiments show that for satisfying full reachability in a road network, given the current assumptions, a connected k-dominating set provides a more desirable solution as both connectivity and reachability are achieved while also providing a lower cardinality solution.

6 Discussion

This section discusses the implications of the findings from Section 5.3, acknowledge certain weaknesses of the research conducted in the thesis, and points to further research that can be viable for future applications.

When allocating charging stations, using real world data is not necessarily sufficient. The reason for this is that real world travel charging demand might not be representative for future charging demand as the means of transportation electrifies. Hence, one aspect of the allocation process must take into account the minimum required infrastructure for facilitating feasible trips and reachability. The connected k-dominating set satisfies the issue of reachability without taking into account the capacity and demand present at each suggested location, which is an aspect that should also be considered in traffic data or simulations. It is also important to note that there is a degree of uncertainty around the optimality of the greedy solutions, and more advanced heuristics can- and should be applied for producing more feasible solutions.

When analyzing the current system, given the reachability thresholds employed in this thesis, it is clear that the current state of the charging station locations is subpar with the proposed solution. As was discussed in Section 4.1, the current required battery capacity for having at least 1 charging station at any given vertex is 98 kWh. However, it is worth noting that this range also accounts for remote locations. Nonetheless, this experiment requires the whole country to be accessible, which yields the current system unfeasible.

For instance, consider the connected k-dominating set $CkDS_{20,2}$ which has a cardinality of 445 vertices. This number is reasonably close to the extrapolated 461 currently existing charging station locations, which makes this set a fairly comparable sample. Figure 6.5 illustrates the $CkDS_{20,2}$ solution and the current system. The main observation concerning the current system is that most charging stations are spatially distributed in clusters around urban areas, while

charging stations outside the urban areas are distributed seemingly at random along the roads. Conversely, the $CkDS_{20,2}$ solution allocates charging stations systematically along the roads without any obvious clusters. It is also clear that the current system is exceptionally inadequate in non- urban areas like the northern and western parts of the country. Increasing the range also increases the spacing between each charging station, thus reducing the size of the solution.

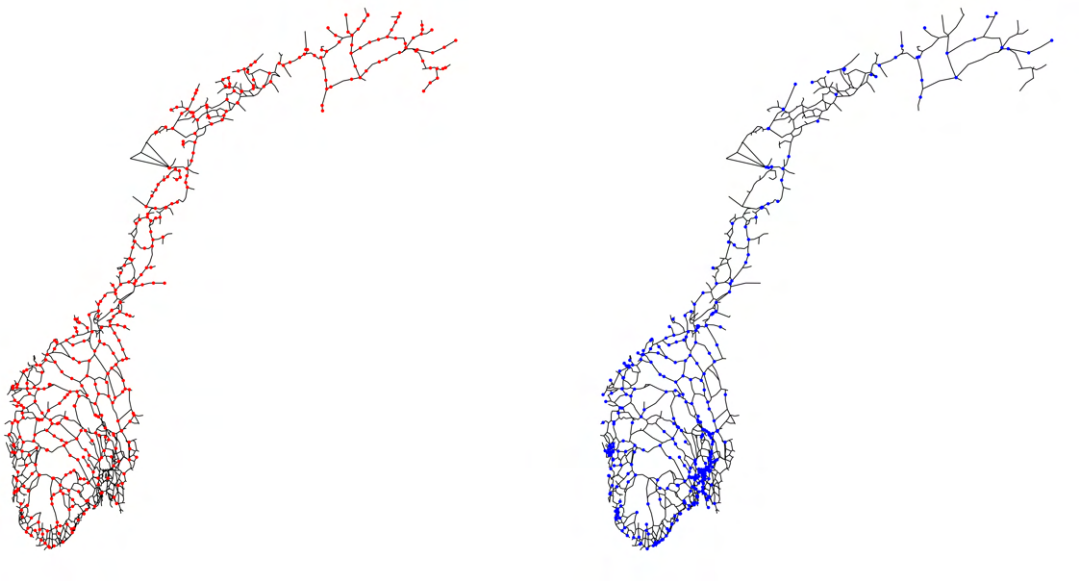

Figure 6.1: $CkDS_{20,2}$ (left) and current system (right)

By performing a Dijkstra search for each tested range[4], the number of neighboring charging stations in the current system for each vertex can be computed. These findings are presented in Table 6.1 below, which shows that the minimum number of adjacent charging stations remains zero across all tested ranges.

Category	Mean nbrs.	Median nbrs.	Min nbrs.	Max nbrs.	St.dev.
20 kWh baseline	21.219	12	0	86	24.084
30 kWh baseline	36.047	18	0	118	37.538
40 kWh baseline	51.391	26	0	144	48.043

Table 6.1: Baseline neighbors for range 20, 30 and 40 kWh

[4]20, 30 and 40 kWh

By using the reachability graphs constructed in Section 4.2, one can compute the coverage of the current system for different battery capacities. Figure 6.2 below maps all vertices in the road network and colors them based on how many charging stations exist within 20 kWh battery capacity. Green vertices have at least 4 charging stations within 20 kWh range, while red vertices have 0. It is evident that the southern parts of the country, especially along the coast, and other urban areas like Trondheim, are well covered with this battery capacity. The northern parts of the country and the mountain ranges in the middle of the country have especially low coverage.

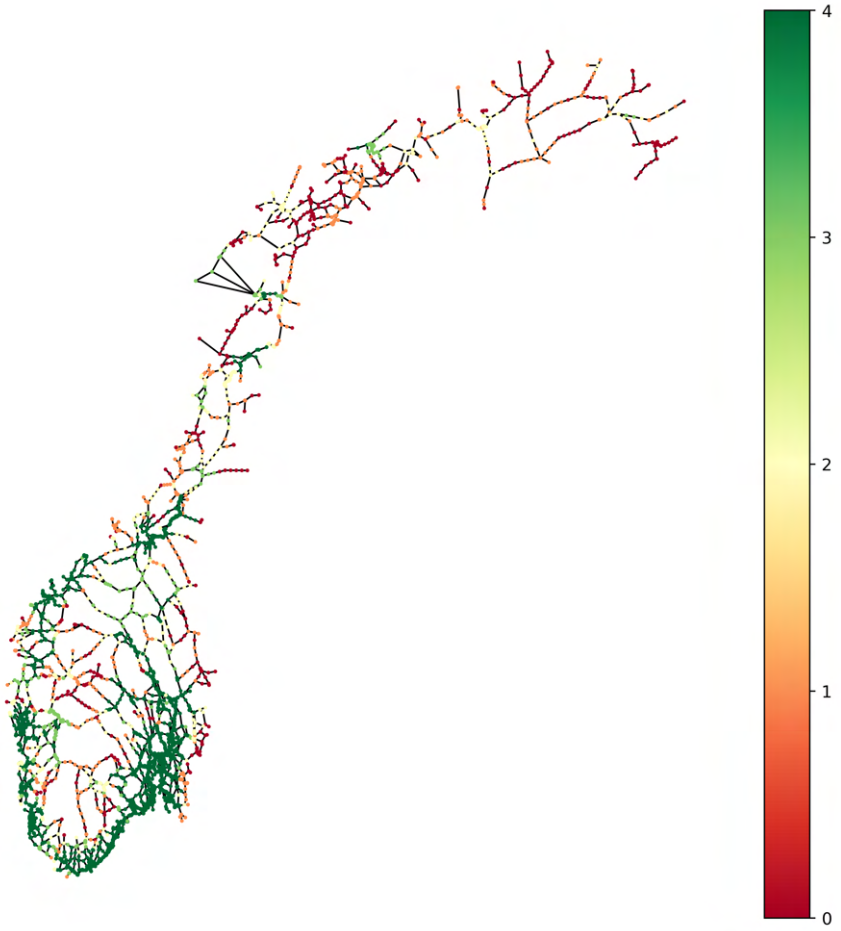

Figure 6.2: Number of charging station within 20 kWh battery capacity

As the battery capacity increases to 30 kWh in Figure 6.3, the coverage increases across the country. However, the problem of coverage in the north and the mountain range persist.

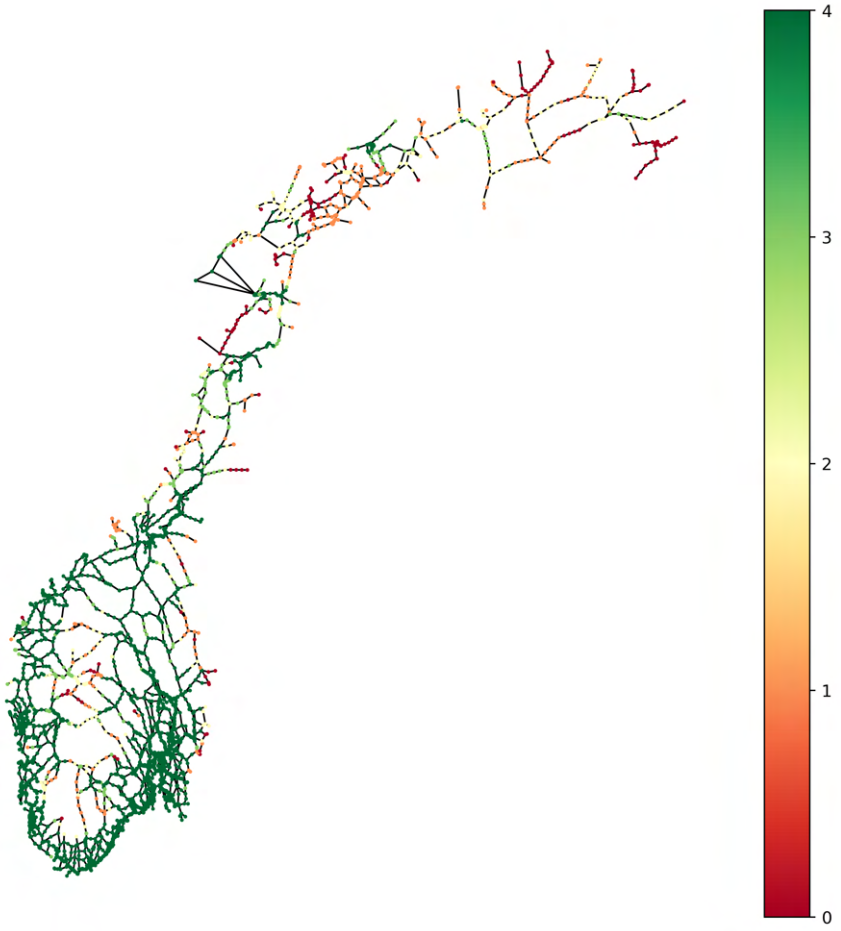

Figure 6.3: Number of charging station within 30 kWh battery capacity

Lastly, when the battery capacity is 40 kWh, as illustrated in Figure 6.4, the mountain ranges in the southern and middle parts of the country are covered. However, many parts of the north have either low or no coverage. These findings emphasize the need of efficient and strategical locating of future fast charging stations, so that more parts of the network can gain coverage.

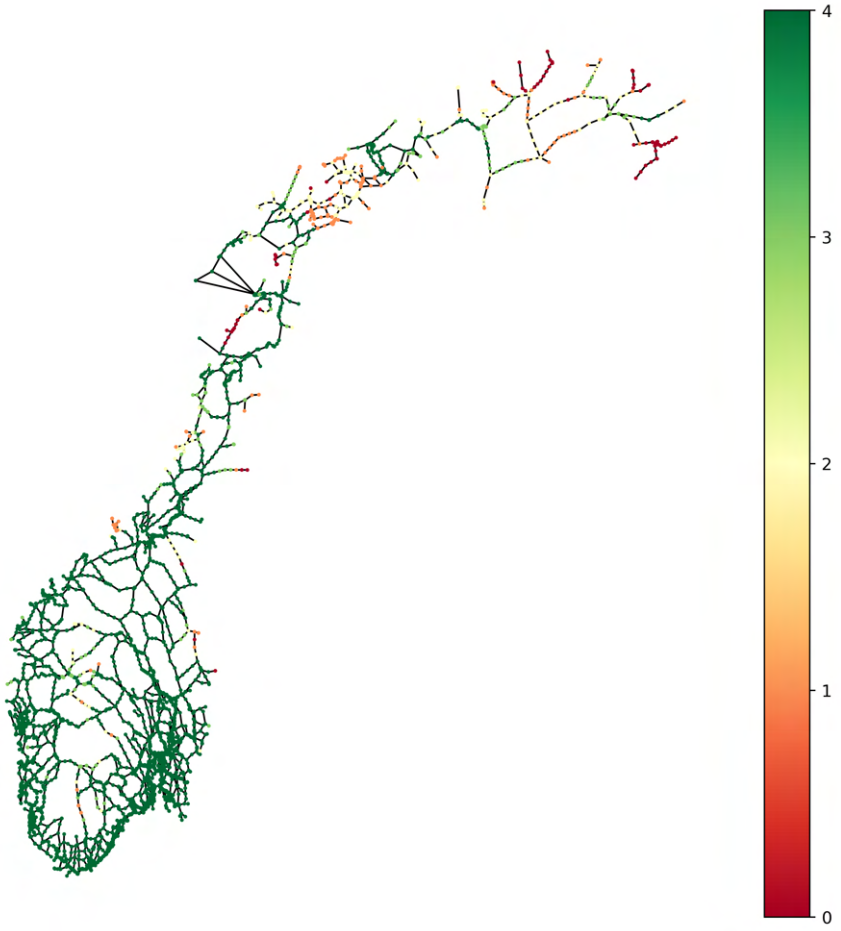

Figure 6.4: Number of charging station within 40 kWh battery capacity

Although no specific metric is used to quantify the deviation from the $CkDS_{20,2}$ solution and the current system, one can get a better overview of the differences in solutions by visualizing the intersection between both sets. Figure 6.5 illustrates $CkDS_{20,2}$ by red vertices, and $CkDS_{20,2} \cap CS$, where CS is the set containing currently existing charging station locations, by blue vertices. From this figure, it is evident that the current system is far from adequate as the number of intersecting nodes is 22. It should be noted that because the optimality of the proposed solution is unknown, this intersection does not necessarily represent the intersection with a global optimal solution.

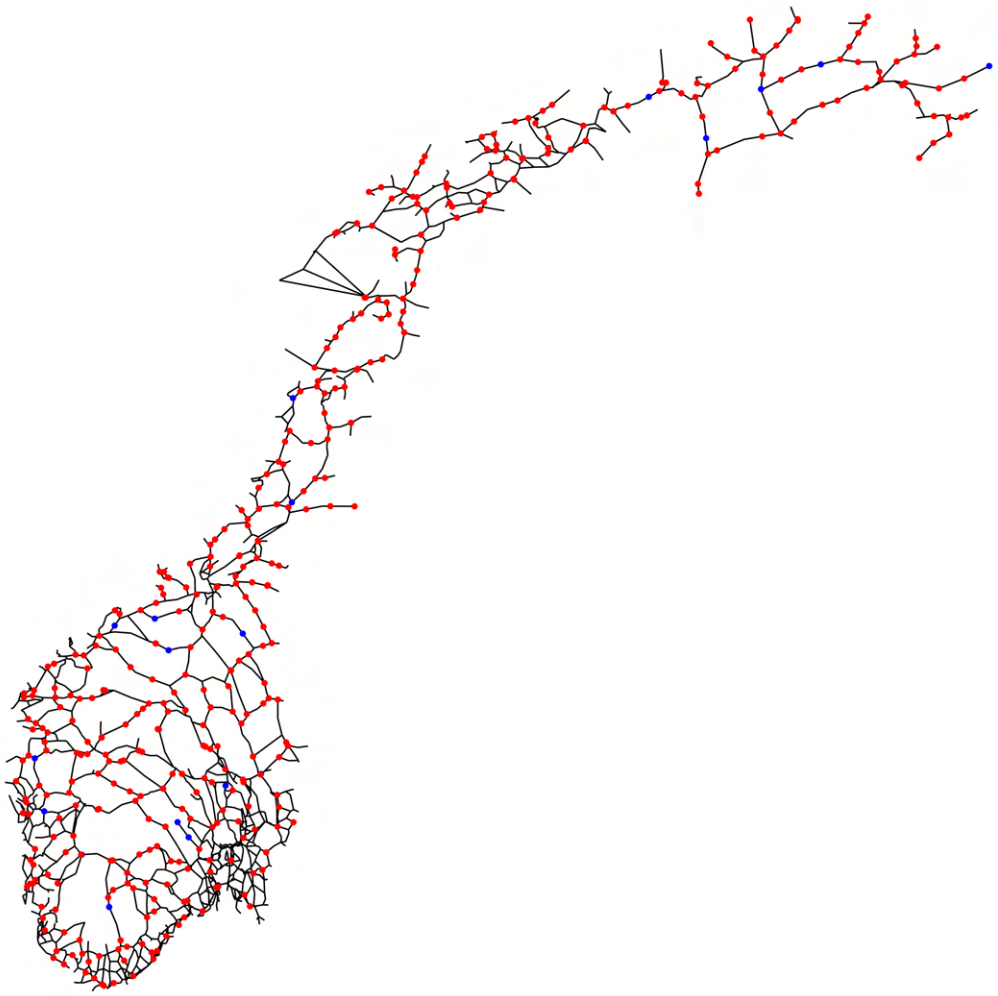

Figure 6.5: $CkDS_{20,2}$ and current system intersection

Which range and k to use when choosing allocation criteria comes down to the policy and decision makers. However, changing these variables have different upsides and downsides associated with them. For instance, a high range will require less infrastructure development (see Figure 5.2) and therefore lower the expenses of the government, municipalities, and companies. Albeit, a higher range moves the transition costs to the consumer because the feasible battery capacity for long distance travel increases, and thus also the price of a vehicle. This can arguably slow the electrification of the transportation sector due to economic barriers to entry. The value for k can also indirectly affect the adoption of electric

vehicles, as a lower value for k can decrease the feasibility of performing long-distance travel due to charging-related detours. A higher k reduces the risk of detours, but increases the required infrastructure.

To exemplify the statements made in the previous paragraph, assume that policymakers want to have drivers to choose between 2, meaning $k = 2$ charging stations within the available range. They are contemplating which range to use as the minimum range threshold, either 20, 30, or 40 kWh. As is presented in figure 6.6 and figure 6.5, the spacing between the charging stations increases as the range threshold increases. Common for all dominating sets is that charging stations are placed in areas where electricity infrastructure is not necessarily present, this is especially visible in *Finnmarksvidda*. Thus, in order to strictly satisfy a $CkDS$ charging station allocation, infrastructure development would have to happen in wildlife areas. However, the necessity of strictly satisfying these conditions in these very remote areas can be questioned depending on the traffic volume.

30 kWh, $k = 2$ 40 kWh, $k = 2$

Figure 6.6: Comparison of 30 and 40 kWh locations for $k = 2$

The current Norwegian government has proposed a 2030 *climate action plan* which, among other things, will rapidly develop country-wide charging infras-

tructure using public and market-based solutions (Norwegian Ministry of Climate and Environment, 2021). This thesis' framework and methodologies can help decision makers successfully plan for where charging stations should be developed to satisfy full reachability given a certain minimum battery capacity and value for k. As argued by Figenbaum and Nordbakke, and mentioned in Section 1, limitations on long distance travel with electric vehicles is one of the last hurdles for mass adoption (Figenbaum, 2019). Thus, a successful deployment of fast charging stations for this exact reason must be a requirement of the government's climate action plan. Further development of charging infrastructure is required in the whole country, but especially in the north of Norway.

6.1 Further Research

The assumptions made place certain limits on the feasibility of the proposed solutions and the methodological framework applied in this thesis.

Firstly, the calculated energy consumption for mobility is based on aggregated data from a vehicle fleet in Japan. While this data certainly has its strengths, such as representing the average energy consumption across different vehicle types, a definite weakness is that it does not account for the Nordic climate and its effect on battery efficiency. For this reason, weather data has not been included in the experiments, as it is already indirectly included in the energy consumption parameters. Hence, a solution which uses battery consumption based off Nordic climate will most likely be able to construct a more representative solution. Alternatively, the temperatures for each vertex location can be retrieved for even more accurate energy consumption estimates. This will be especially important for the northernmost and high altitude regions, as low temperatures are more likely to have a significant impact on the battery capacity.

Secondly, the proposed methodology for allocating charging stations does not account for the charging demand at each candidate location. Therefore, the proposed solutions are only indicative of where **at least** one charging station should

be located. For instance, if origin-destination data is available or charging demand along paths can somehow be obtained through estimation or simulations, one option can be to employ the *CFRLM* from Section 2.2 with the *CkDS* vertices as candidate locations.

Lastly, as previously mentioned in this section, there is uncertainty regarding the optimality of the proposed solutions as this thesis' experiments employed a deterministic greedy algorithm, meaning the proposed solution can be located in a local optima rather than a global one. Hence, one improvement point is to use more advanced heuristics for constructing more desirable solutions.

7 Conclusion

This thesis has explored how an optimal allocation of charging stations can be performed in Norway for 20, 30, and 40 kWh battery capacity using data containing estimated battery consumption and elevation. The experiment finds that for guaranteeing reachability across the entire road network, the use of connected k-dominating sets is better suited than a k-dominating set. This is because the connected k-dominating set guarantees that all vertices, even those in the dominating set, are adjacent to at least one charging station. A connected k-dominating set can be found using the Greedy Connected k-Dominating Set algorithm, which can find a deterministic solution on large graphs within a reasonable time frame. The optimality of this solution is unknown, and additional heuristics can and should be employed or added to improve the solution size.

Furthermore, a comparison of the current charging station, disregarding the proprietary charging infrastructure, and the proposed solution with the minimum range requirement show that there are large improvements to be made in infrastructure development across the entire country. However, the most notable gaps in coverage are present in non- urban areas, with most coverage lacking in the northern parts of the country.

Although moving existing charging stations is not an option, these findings can help national and regional policymakers determine where to prioritize the future development of charging infrastructure so that reachability is satisfied or maximized. In turn, this can increase the feasibility of owning an electric vehicle and thus push the adoption rate forward.

References

Alfred, W. (1929). Theory of The Location of Industries. *University of Chicago Press*.

Bakhshesh, D., Farshi, M., & Hasheminezhad, M. (2017, February). Complexity results for k-domination and α-domination problems and their variants. *arXiv:1702.00533 [cs, math]*. Retrieved 2021-03-22, from http://arxiv.org/abs/1702.00533 (arXiv: 1702.00533)

Boeing, G. (2021). *gboeing/osmnx: OSMnx: Python for street networks. Retrieve, model, analyze, and visualize street networks and other spatial data from OpenStreetMap.* Retrieved 2021-05-27, from https://github.com/gboeing/osmnx

Bouguerra, S., & Bhar Layeb, S. (2019, September). Determining optimal deployment of electric vehicles charging stations: Case of Tunis City, Tunisia. *Case Studies on Transport Policy*, *7*(3), 628–642.

Chung, S. H., & Kwon, C. (2015, April). Multi-period planning for electric car charging station locations: A case of Korean Expressways. *European Journal of Operational Research*, *242*(2), 677–687. Retrieved 2021-01-29, from http://www.sciencedirect.com/science/article/pii/S0377221714008509 doi: 10.1016/j.ejor.2014.10.029

Correa, E., Steiner, M. T., Freitas, A., & Carnieri, C. (2004). A Genetic Algorithm for Solving a Capacitated p-Median Problem. *undefined*. Retrieved 2021-05-27, from /paper/A-Genetic-Algorithm-for-Solving-a-Capacitated-Correa-Steiner/a80ab308768e8d446e00e64f515c4042f84f77b4

Daskin, M. S., & Maass, K. L. (2015). The p-Median Problem. In G. Laporte, S. Nickel, & F. Saldanha da Gama (Eds.), *Location Science* (pp. 21–45). Cham: Springer International Publishing. Retrieved 2021-05-27, from https://doi.org/10.1007/978-3-319-13111-5_2 doi: 10.1007/978-3-319-13111-5_2

Efthymiou, D., Chrysostomou, K., Morfoulaki, M., & Aifantopoulou, G. (2017, June). Electric vehicles charging infrastructure location: a genetic algorithm

approach. *European Transport Research Review*, *9*(2), 1–9.

Figenbaum, E. (2019). Battery electric vehicle user experiences in Norway's maturing market.

Fink, J. F., & Jacobson, M. S. (1985, September). n-Domination in graphs. In *Graph theory with applications to algorithms and computer science* (pp. 283–300). USA: John Wiley & Sons, Inc.

Fu, D., Han, L., Yang, Z., & Jhang, S. T. (2016, July). A Greedy Algorithm on Constructing the Minimum Connected Dominating Set in Wireless Network. *International Journal of Distributed Sensor Networks*, *12*(7), 1703201. Retrieved 2021-04-30, from https://doi.org/10.1177/155014771703201 (Publisher: SAGE Publications) doi: 10.1177/155014771703201

Funke, S., Nusser, A., & Storandt, S. (2015, August). Placement of Loading Stations for Electric Vehicles: No Detours Necessary! *Journal of Artificial Intelligence Research*, *53*, 633–658.

Gagarin, A., & Corcoran, P. (2018, August). Multiple domination models for placement of electric vehicle charging stations in road networks. *Computers & Operations Research*, *96*, 69–79.

GeoNorge. (2021). *National roads database - road network for routing - Kartkatalogen.* Retrieved 2021-03-09, from https://kartkatalog.geonorge.no/metadata/statens-vegvesen/nvdb-ruteplan-nettverksdatasett/8d0f9066-34f9-4423-be12-8e8523089313

Hakimi, S. L. (1964, June). Optimum Locations of Switching Centers and the Absolute Centers and Medians of a Graph. *Operations Research*, *12*(3), 450–459.

Hansberg, A. (2010, July). Bounds on the connected k-domination number in graphs. *Discrete Applied Mathematics*, *158*(14), 1506–1510. Retrieved 2021-04-30, from https://www.sciencedirect.com/science/article/pii/S0166218X10002039 doi: 10.1016/j.dam.2010.05.021

He, Y., Kockelman, K. M., & Perrine, K. A. (2019, March). Optimal locations of U.S. fast charging stations for long-distance trip completion by battery electric vehicles. *Journal of Cleaner Production*, *214*, 452–461.

Hodgson, M. J. (1990). A Flow-Capturing Location-Allocation Model. *Geographical Analysis*, *22*(3), 270–279.

Jochem, P., Szimba, E., & Reuter-Oppermann, M. (2019, August). How many fast-charging stations do we need along European highways? *Transportation Research Part D: Transport and Environment*, *73*, 120–129.

Kim, J.-G., & Kuby, M. (2012, March). The deviation-flow refueling location model for optimizing a network of refueling stations. *International Journal of Hydrogen Energy*, *37*(6), 5406–5420.

Kuby, M., & Lim, S. (2005, June). The flow-refueling location problem for alternative-fuel vehicles. *Socio-Economic Planning Sciences*, *39*(2), 125–145.

Lam, A. Y. S., Leung, Y., & Chu, X. (2014, November). Electric Vehicle Charging Station Placement: Formulation, Complexity, and Solutions. *IEEE Transactions on Smart Grid*, *5*(6), 2846–2856.

Lim, S., & Kuby, M. (2010, July). Heuristic algorithms for siting alternative-fuel stations using the Flow-Refueling Location Model. *European Journal of Operational Research*, *204*(1), 51–61.

Liu, B., Wang, W., Kim, D., Li, D., Wang, J., Tokuta, A. O., & Jiang, Y. (2016, October). On Approximating Minimum 3-Connected m-Dominating Set Problem in Unit Disk Graph. *IEEE/ACM Transactions on Networking*, *24*(5), 2690–2701. (Conference Name: IEEE/ACM Transactions on Networking) doi: 10.1109/TNET.2015.2475335

Liu, K., Yamamoto, T., & Morikawa, T. (2017, July). Impact of road gradient on energy consumption of electric vehicles. *Transportation Research Part D: Transport and Environment*, *54*, 74–81. Retrieved 2021-03-04, from `https://www.sciencedirect.com/science/article/pii/S1361920917303887` doi: 10.1016/j.trd.2017.05.005

Ministry of Transport. (2017, April). *Meld. St. 33 (2016–2017)* [Stortingsmelding]. Retrieved 2020-10-30, from `https://www.regjeringen.no/no/dokumenter/meld.-st.-33-20162017/id2546287/` (Publisher: regjeringen.no)

Muttaqin, P. S., Finata, R. A., & Masturo, A. A. (2020). Facility Location Model for Emergency Humanitarian Logistics Using Set Covering and Analytic Network Process (ANP) Method. *undefined*. Retrieved 2021-05-27, from /paper/A-Genetic-Algorithm-for-Solving-a-Capacitated-Correa-Steiner/a80ab308768e8d446e00e64f515c4042f84f77b4

Norwegian Ministry of Climate and Environment. (2016, June). *Norway has ratified the Paris Agreement* [Nyhet]. Retrieved 2020-10-29, from https://www.regjeringen.no/en/aktuelt/norge-har-ratifisert-parisavtalen/id2505365/ (Publisher: regjeringen.no)

Norwegian Ministry of Climate and Environment. (2021, January). *Norway's comprehensive climate action plan* [Nyhet]. Retrieved 2021-05-22, from https://www.regjeringen.no/en/aktuelt/heilskapeleg-plan-for-a-na-klimamalet/id2827600/ (Publisher: regjeringen.no)

OpenChargeMap. (2021, April). *openchargemap/ocm-data.* Open Charge Map. Retrieved 2021-04-16, from https://github.com/openchargemap/ocm-data (original-date: 2020-03-10T03:45:12Z)

Owen, S. H., & Daskin, M. S. (1998, December). Strategic facility location: A review. *European Journal of Operational Research*, *111*(3), 423–447.

Pagany, R., Camargo, L. R., & Dorner, W. (2019, July). A review of spatial localization methodologies for the electric vehicle charging infrastructure. *International Journal of Sustainable Transportation*, *13*(6), 433–449.

Rangnes, H.-K. (2020, August). *Sommerens elbilferie: Ladere ute av drift og lange køer.* Retrieved 2020-10-29, from https://www.nrk.no/vestfoldogtelemark/sommerens-elbilferie_-ladere-ute-av-drift-og-lange-koer-1.15128900

Statistics Norway. (2020a). *07849: Registered vehicles, by type of transport and type of fuel (M) 2008 - 2019.* Retrieved 2020-10-29, from http://www.ssb.no/en/statbanken/statbank/table/07849/

Statistics Norway. (2020b). *08940: Greenhouse gases, by source, energy product and pollutant 1990 - 2019.* Retrieved 2020-10-29, from http://www.ssb.no/en/statbanken/statbank/table/08940/

Upchurch, C., & Kuby, M. (2010, November). Comparing the p-median and flow-refueling models for locating alternative-fuel stations. *Journal of Transport Geography*, *18*(6), 750–758.

Upchurch, C., Kuby, M., & Lim, S. (2009). A Model for Location of Capacitated Alternative-Fuel Stations. *Geographical Analysis*, *41*(1), 85–106.

Appendices

A Link to source data and GitHub repository

Data used for extracting the road network can be retrieved from GeoNorge through the following URL:

`https://kartkatalog.geonorge.no/metadata/statens-vegvesen/nvdb-ruteplan-nettverksdatasett/8d0f9066-34f9-4423-be12-8e8523089313`

The source code of this thesis is located in the author's GitHub repository:

`https://github.com/samuelberntzen/Optimal-Allocation-of-Electric-Vehicle-Charging-Stations-A-case-study-of-the-Norwegian-road-network`